Formation and Structure of Coordinatively Unsaturated Cp*Ir–Amino Acid Complexes. Kinetic and Thermodynamic Control in Highly Diastereoselective Complexation Reactions

D. B. Grotjahn* and T. L. Groy†

Department of Chemistry and Biochemistry, Box 871604, Arizona State University, Tempe, Arizona 85287-1604

Received January 17, 1995®

Amino acid derivatives bearing an electron-withdrawing group Z on N (Z = tosyl, CO_2CH_2Ph, or acetyl) serve as (N,O)-chelating, dianionic ligands to the fragment Cp*Ir. Six such complexes have been prepared, all of them coordinatively unsaturated yet air-stable. The structure of the *N*-tosylglycine derivative $C_{19}H_{24}IrNO_4S$ (**5a**) was analyzed at 20 °C. A planar chelate ring was revealed, and relatively short Ir–N and Ir–O bonds suggested stabilization of unsaturated Ir by π-donation. Crystals of the (*R*)-*N*-tosylphenylglycine complex $C_{25}H_{28}IrNO_4S$ (**5f**) were monoclinic. Some distortion of the chelate ring was seen, and both aryl rings were syn, the angle between their mean planes being 19°. Within seconds, red solutions of the unsaturated complexes **5** turn yellow on addition of ligands such as phosphines, CO, and primary aliphatic or heterocyclic amines. Ligands add to chiral complexes so as to place the amino acid side chain R and Cp* cis to each other on the metallacycle, suggesting preferred approach of the ligand to **5** from the side opposite R. For one PMe_3 adduct this was shown to be the result of kinetic control (≥50:1 selectivity at 25 °C) and thermodynamic control (40:1 selectivity after equilibration at 90 °C, half-life = 5 h). PPh_3 and amines exchange within minutes at 25 °C. The stereoselectivity of ligand addition was highest for smaller ligands. Comparing this result and previous work suggests that steric interactions between added ligand and the amino acid side chain R determine diastereoselectivity.

Introduction

Amino acid–metal complexes have been the subject of innumerable studies,[1] prompted by the role of metals in biochemistry[2] and by the role of amino acids in producing chiral catalysts.[3] Transformation of amino acids into valuable enantiomerically pure organic compounds using organic reagents or main-group organometallics[4] are useful, but conversions using transition-metal catalysts or reagents appear to be unknown, motivating the following studies.

With very few exceptions,[5] amino acid-metal complexes[1,6] are coordinatively saturated. For example, interaction of N-unsubstituted amino acid salts **1** with $[Cp^*IrCl(\mu\text{-}Cl)]_2$ (**2**) leads to 18-electron complexes **3** (eq 1), the stereogenic element of the amino acid producing

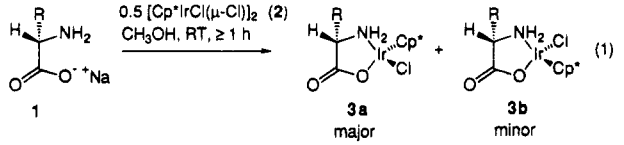

mixtures modestly enriched in diastereomer **3a** (from 50:50 up to 92:8).[6a,b] Here we report in full[7] that, under modified conditions, amino acid derivatives **4** (Scheme 1) bearing electron-withdrawing groups Z on N afford air-stable 16-electron species **5**, two members of which are characterized by X-ray diffraction. Furthermore, unlike ligand substitutions on **3** and related species, ligand *addition* reactions of chiral **5** proceed with high (≥25:1) stereoselectivity. Additional experiments reported here define the range of ligands that bind to **5** and demonstrate the operation of kinetic and thermodynamic control in ligand binding, critical considerations in the design and use of asymmetric catalysts related to **4**.[8]

Results

Synthesis of 5a–f and Crystallography of 5a and 5f. Our initial goal was to attach an amino acid to a

† X-ray crystal structures.

® Abstract published in *Advance ACS Abstracts,* June 1, 1995.

(1) (a) Laurie, S. H. Amino Acids, Peptides and Proteins. In *Comprehensive Coordination Chemistry*; Wilkinson, G., Ed.; Pergamon: Oxford, 1987, Vol. 2, pp 739–776. (b) Ioganson, A. A. *Russ. Chem. Rev.* **1985**, *54*, 277–292. (c) Sigel, H.; Martin, R. B. *Chem. Rev.* **1982**, *82*, 385–426.

(2) Metalloproteins: Structural Aspects. *Adv. Prot. Chem.* **1991**, *42*. Ibers, J. A.; Holm, R. H. *Science* **1980**, *209*, 223–235.

(3) (a) Brunner, H. *Top. Stereochem.* **1988**, *18*, 129–247. (b) *Chiral Catalysis; Asymmetric Synthesis;* Morrison, J., Ed.; Academic: Orlando, 1985; Vol. 5. (c) *Asymmetric Catalysis in Organic Synthesis*; Noyori, R., Ed.; Wiley: New York, 1994. (d) *Catalysis in Asymmetric Synthesis*; Ojima, I., Ed.; VCH: New York, 1993.

(4) (a) Reetz, M. T. *Angew. Chem., Int. Ed. Engl.* **1991**, *30*, 1531–1546. (b) Scott, J. W. Readily Available Chiral Carbon Fragments and Their Use in Synthesis. In *Asymmetric Synthesis*; Morrison, J. D., Scott, J. W., Eds.; Academic: Orlando, 1984; Vol. 4, pp 1–226.

(5) (a) To our knowledge, the only coordinatively unsaturated amino acid complexes reported are $(CO)_2Rh^I$(amino acidato) complexes, which undergo CO substitution by PR_3 and AsR_3: Dowerah, D.; Singh, M. M. *J. Indian Chem. Soc.* **1980**, *57*, 368–371. Dowerah, D.; Singh, M. M. *J. Chem. Res., Synop.* **1979**, 38. Dowerah, D.; Singh, M. M. *Transition Met. Chem. (London)* **1976**, *1*, 294–295. (b) A dimeric Cp*Rh–glycine *amide* complex (**16**) was recently suspected on the basis of ^1H NMR evidence of undergoing partial monomerization in solution to a species related to **5** (but formulated as rapidly epimerizing at Rh, **17a** + **17b**): Krämer, R.; Polborn, K.; Robl, C.; Beck, W. *Inorg. Chim. Acta* **1992**, *198–200*, 415–420.

0276-7333/95/2314-3669$09.00/0

Scheme 1

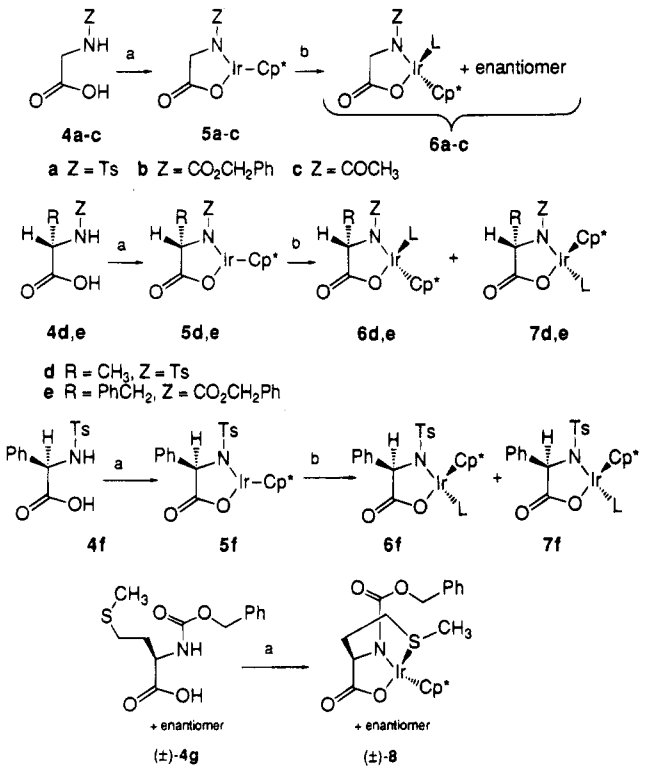

[a] Legend: (a) K_2CO_3, $[Cp^*IrCl(\mu\text{-}Cl)]_2$, THF, or CH_3CN, room temperature, 4–36 h; (b) ligand, $CDCl_3$ or C_6D_6, room temperature, ≤15 s.

metal as a chelating, dianionic ligand, which was anticipated to bind strongly to the metal center. Deprotonation at N was to be facilitated by N-substitution with an electron-withdrawing group Z,[1] as in sulfonamides, amides, and carbamates **4**. Reported reactions of **2** and N-unsubstituted amino acid salts **1** were conducted in alcohol solvents.[6a] However, because amide and sulfonamide anions exhibit greater basicity in aprotic media,[9] and because hydrogen bonding attenuates nucleophilicity of anionic species,[10] we employed nonprotic media (THF or CH_3CN) in reactions of **2** and amino acid derivatives **4**[11] with the expectation that the coordination sphere of the metal in the product (**6** or **7**, L = THF or CH_3CN) would include a solvent molecule, which could be easily displaced as desired with other ligands. Thus, a nitrogen-saturated mixture of **4a**, dimer **2**,[12] and anhydrous K_2CO_3 (molar ratio 1.00:0.50:2.0–3.0) in THF (initial orange color) was stirred for 24 h, during which time the color deepened to red. The residue remaining after rotary evaporation was diluted with CH_2Cl_2 and filtered through Celite, and the filtrate was concentrated to afford a red foam in high yield. Similar results were obtained using CH_3CN as solvent, although before turning red the mixture initially was yellow, presumably due to dissolution of **2** with formation of $Cp^*Ir(Cl)_2(CH_3CN)$.[13]

Analytical data for the reaction product from **4a** (Tables 1–3) pointed to chelation of the amino acid derivative: deprotonation at N was implicated by a ^1H NMR spectrum featuring a two-proton singlet, ascribable to the methylene protons, and deprotonation at both N and O was apparent from a lack of infrared absorption above 3100 cm^{-1}. Furthermore, all analytical data, including elemental analysis, were consistent with the absence of coordination by reaction solvents THF or CH_3CN, or even by N_2 in the product, suggesting structure **5a**. However, the geometry at Ir remained unclear. Even at −90 °C, the ^1H NMR spectrum of **5a** in CD_2Cl_2 revealed a sharp two-proton singlet at δ 3.20 ppm for the methylene group, consistent with either an achiral structure or rapidly interconverting, enantiomeric, octahedral structures. Thus, the structural ambiguity surrounding **5a** was settled by X-ray crystallographic analysis (Figure 1 and Tables 4, 10, and 11) on a crystal readily obtained by vapor diffusion of petroleum ether into a hot, undeoxygenated toluene solution of the compound. The planarity of the metallacycle is revealed by the position of the centroid of Cp* only 0.022 Å away from the mean plane defined by the five atoms of the chelate ring. Furthermore, no atom of the chelate lies more than 0.029 Å away from the metallacycle mean plane. Compared with 18-electron **3**,[6a,b] the Ir–N and Ir–O bonds are ca. 0.15 and 0.06 Å shorter, respectively, suggesting stabilization of the formally 16-electron metal by lone pairs on N and O, as proposed by Bergman and co-workers[14] in their structural analysis of **9**. Additional evidence for π-donation from N and O[15,16] in **5** will be discussed below. The other metrical parameters for **5a**, in particular, the length of the carboxylato C–O double and single bonds,

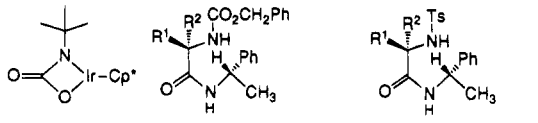

(6) (a) Krämer, R.; Polborn, K.; Wanjek, H.; Zahn, I.; Beck, W. *Chem. Ber.* **1990**, *123*, 767–778. (b) Carmona, D.; Mendoza, A.; Lahoz, F. J.; Oro, L. A.; Lamata, M. P.; San Jose, E. *J. Organomet. Chem.* **1990**, *396*, C17–C21. For amino acid chelate complexes to other organometallic fragments, see: (c) Dersnah, D. F.; Baird, M. C. *J. Organomet. Chem.* **1977**, *127*, C55–C58. (d) Sheldrick, W. S.; Heeb, S. *J. Organomet. Chem.* **1989**, *377*, 357–366. (e) Sheldrick, W. S.; Exner, R. *Inorg. Chim Acta* **1990**, *175*, 261–268. (f) Werner, H.; Daniel, T.; Nürnberg, O.; Knaup, W.; Meyer, U. *J. Organomet. Chem.* **1993**, *445*, 229–235. (g) Sheldrick, W. S.; Gleichmann, A. *J. Organomet. Chem.* **1994**, *470*, 183–187. (h) Lippmann, E.; Krämer, R.; Beck, W. *J. Organomet. Chem.* **1994**, *466*, 167–174. (i) Bergs, R.; Sünkel, K.; Beck, W. *Chem. Ber.* **1993**, *126*, 2429–2432. (j) Shinoda, S.; Inoue, N.; Takita, K.; Saito, Y. *Inorg. Chim. Acta* **1982**, *65*, L21–L23. (k) Darensbourg, D. J.; Atnip, E. V.; Klausmeyer, K. K.; Reibenspies, J. H. *Inorg. Chem.* **1994**, *33*, 5230–5237. Cp_2Ti(amino acid)$_2$ complexes: (l) Klapötke, T. M.; Köpf, H.; Tornieporth-Oetting, I. C.; White, P. S. *Angew. Chem., Int. Ed. Engl.* **1994**, *33*, 1518–1519. Klapötke, T. M.; Köpf, H.; Tornieporth-Oetting, I. C.; White, P. S. *Organometallics* **1994**, *13*, 3628–3633.

(7) Grotjahn, D. B.; Groy, T. L. *J. Am. Chem. Soc.* **1994**, *116*, 6969–6970.

(8) Deloux, L.; Srebnik, M. *Chem. Rev.* **1993**, *93*, 763–784 and references therein.

(9) Bordwell, F. G. *Acc. Chem. Res.* **1988**, *21*, 456–463. Dyumaev, K. M.; Korolev, B. A. *Russ. Chem. Rev.* **1980**, *49*, 1021–1032.

(10) March, J. *Advanced Organic Chemistry*, 4th ed.; Wiley: New York, 1992; p 349ff.

(11) Compounds **4b**, **4c**, and **4e** were purchased. N-Ts derivatives **4a** and **4d** (**4f** was made using a similar procedure): McChesney, F. W.; Swann, W. K. Jr. *J. Am. Chem. Soc.* **1937**, *59*, 1116–1118. (±)-**4g**: Dekker, C. A.; Fruton, J. S. *J. Biol. Chem.* **1948**, *173*, 471–477.

(12) White, C.; Yates, A.; Maitlis, P. M. *Inorg. Synth.* **1992**, *29*, 228.

(13) For CH_3CN and $[(COD)Ir(\mu\text{-}Cl)]_2$, see: Day, V. W.; Klemperer, W. G.; Main, D. J. *Inorg. Chem.* **1990**, *29*, 2345–2355.

(14) Glueck, D. S.; Wu, J.; Hollander, F. J.; Bergman, R. G. *J. Am. Chem. Soc.*, **1991**, *113*, 2041–2054.

(15) (a) Goldman, A. S.; Halpern, J. *J. Organomet. Chem.* **1990**, *382*, 237–253. (b) Lunder, D. M.; Lobkovsky, E. B.; Streib, W. E.; Caulton, K. G. *J. Am. Chem. Soc.* **1991**, *113*, 1837–1838.

Table 1. Yield, Color, Melting Points,[a] IR Data, and Elemental Analyses of Complexes Isolated

product	yield[b] (%)	appearance	IR $\nu_{C=O}$ (cm^{-1})	molecular formula (molecular wt)	anal. calcd, % C	H	N	anal. found, % C	H	N
5a	97	red foam	1684 (CH_2Cl_2, NaCl) 1684 (KBr)	$C_{19}H_{24}IrNO_4S$ (554.70)	41.14	4.36	2.53	41.95	4.47	2.38
5b	94	deep red solid[c]	1682, 1672 (KBr)	$C_{20}H_{24}IrNO_4$ (534.62)	44.93	4.52	2.62	44.40	4.44	2.61
5c[d]	96	yellow solid	1653, 1570, 1553 (KBr) 1659, 1642 (CH_2Cl_2, NaCl)	$(C_{14}H_{20}IrNO_3)_n$ (n × 442.54)	38.00	4.52	3.17	38.17	4.83	2.64
5d[e]	100	deep red powder	1678 (KBr)	$C_{20}H_{26}IrNO_4S$ (568.73)	42.24	4.61	2.46	42.46	4.79	2.25
5e	96	deep red solid[f]	1681, 1653 (KBr) 1668 (CH_2Cl_2, NaCl)	$C_{27}H_{30}IrNO_4$ (624.76)	51.91	4.84	2.24	52.38	4.98	2.20
5f	96	red foam[g]	1674 (KBr)	$C_{25}H_{28}IrNO_4S$ (630.79)	47.60	4.47	2.22	47.51	4.58	2.26
6a–PMe_3	89	yellow powder[h]	1650 (KBr)	$C_{22}H_{33}IrNO_4PS$ (630.77)	41.89	5.27	2.22	42.05	5.31	2.10
6b–PMe_3[i]			1645 (CH_2Cl_2, NaCl)							
6d–PMe_3	95	pale yellow solid	1644 (KBr)	$C_{23}H_{35}IrNO_4PS$ (640.80)	42.84	5.47	2.17	42.58	5.48	1.97
6e–PMe_3[i]			1637 ($CDCl_3$, NaCl)							
7e–PMe_3	60	pale yellow crystals	1648 (KBr)	$C_{30}H_{39}IrNO_4P$ (700.84)	51.41	5.61	2.00	51.34	5.63	2.04
6d–PMe_2Ph	100	pale yellow powder	1651 (KBr)	$C_{28}H_{37}IrNO_4PS$ (706.86)	47.58	5.27	1.98	46.67	5.32	1.94
6d–$PMePh_2$	92	yellow powder	1653 (KBr)	$C_{33}H_{39}IrNO_4PS$ (768.94)	51.55	5.11	1.82	51.64	5.19	1.83
6a–PPh_3	97	yellow powder	1661 (KBr)	$C_{37}H_{39}IrNO_4PS$ (816.99)	54.50	4.81	1.71	54.21	4.86	1.66
6d–PPh_3[j]	88	yellow powder	1647 (KBr)	$C_{38}H_{41}IrNO_4PS$ (831.01)	54.92	4.97	1.69	53.87	4.97	1.90
6a–CO	100	pale yellow powder	2033,[k] 1671 (KBr)							
6d–CO	90	pale yellow powder	2042,[k] 1669 (KBr)							
(±)-**6d**–DMAP	100	pale yellow solid	1643 (KBr)	$C_{27}H_{37}IrN_3O_4S$ (691.90)	46.87	5.39	6.07	46.88	5.34	5.97
6a–MeIm[i,l]			1625 ($CDCl_3$, NaCl)							
(±)-**8**	98	yellow solid	1641 (br, KBr)	$C_{23}H_{32}IrNO_4S$ (610.81)	45.23	5.28	2.29	45.49	5.16	2.18

[a] In N_2-filled, sealed capillaries. All compounds examined decomposed upon melting at temperatures dependent on how long sample was heated. Temperatures reported are for samples heated from 5–10 degrees below reported values. [b] Yields refer to material characterized by elemental analysis. [c] Mp 145–148 °C (decomp). [d] Structure in solution, see text. [e] Racemate obtained in 90% yield, exhibited identical spectral properties. [f] Mp 155–158 °C (decomp). [g] Mp 210°C (decomp). [h] Mp 225 °C (decomp). [i] Not isolated. [j] Presumed to be admixed with **7d**–PPh_3. [k] $\nu_{C=O}$. [l] MeIm = 1-methylimidazole.

are unexceptional. The nearest intermolecular contacts for the metal center are a carbonyl oxygen in a symmetry-related molecule at 5.47 Å, securing the assignment that in **5a** the metal center interacts only with the Cp* and amino acid chelate ligands, both in solution and in the crystal.

Eventually, using similar synthetic procedures, other examples of complexes **5** were obtained as red solids or foams in ≥94% yield. Evidence presented below indicates that in these systems, red color is diagnostic for coordinative unsaturation. Products **5** are air-stable but solutions lose their red color when in contact with water, and chromatography of **5** over SiO_2 seems to destroy the complexes, presumably by hydrolysis. Occasionally in the synthesis of **5c** in THF the addition of Na_2SO_4 was required to achieve a red color, suggesting that water presumably produced in the neutralization of acid by carbonate ion interferes with the formation of **5c**. Alkoxide and amide ligands on late transition metals have been observed to act as hydrogen-bond acceptors,[15,17] and can exchange with the hydrogen bond donor.[15,17]

Base-catalyzed epimerization of amino acid derivatives can be a serious problem in peptide synthesis.[18] Therefore, evidence for the enantiomeric purity of chiral **5** was sought. The high susceptibility of phenylglycine derivatives to base-catalyzed racemization[19] suggested that the enantiomeric purity of **5f** would be an especially stringent test. Unfortunately, the application of chiral lanthanide shift reagents[20] led only to broadening of resonances in the ^1H NMR spectrum of chiral **5**. However, derivatization of the amino acid ligand in **5e**

(16) Reviews: (a) Bryndza, H. E.; Tam, W. *Chem. Rev.* **1988**, *88*, 1163–1188. (b) Fryzuk, M. D.; Montgomery, C. D. *Coord. Chem. Rev.* **1989**, *95*, 1–40. Alkoxide π-donation: (c) Hubbard, J. L.; McVicar, W. K. *Inorg. Chem.* **1992**, *31*, 910–913. (d) Poulton, J. T.; Sigalas, M. P.; Folting, K.; Streib, W. E.; Eisenstein, O.; Caulton, K. G. *Inorg. Chem.* **1994**, *33*, 1476–1485. (e) Bickford, C. C.; Johnson, T. J.; Davidson, E. R.; Caulton, K. G. *Inorg. Chem.* **1994**, *33*, 1080–1086. Amide complexes: (f) Villanueva, L. A.; Abboud, K. A.; Boncella, J. M. *Organometallics* **1994**, *13*, 3921–3931. (g) Rahim, M.; Ahmed, K. J. *Organometallics*, **1994**, *13*, 1751–1756. (h) Dewey, M. A.; Knight, D. A.; Arif, A.; Gladysz, J. A. *Chem. Ber.* **1992**, *125*, 815–824 and references therein. Amide complexes in which there appears to be no π-donation: (i) Joslin, F. L.; Johnson, M. P.; Mague, J. T.; Roundhill, D. M. *Organometallics* **1991**, *10*, 2781–2794.

(17) Simpson, R. D.; Bergman, R. G. *Organometallics* **1993**, *12*, 781–796.

(18) Kemp, D. S. In *The Peptides*; Gross, E., Meienhofer, J., Eds.; Academic: New York, 1979; Vol. 1, pp 315–383.

(19) Carpino, L. *J. Org. Chem.* **1988**, *53*, 875–878. Stroud, E. D.; Fife, D. J.; Smith, G. G. *J. Org. Chem.* **1983**, *48*, 5368–5369. Smith, G. G.; Sivakua, T. *J. Org. Chem.* **1983**, *48*, 627–634.

(20) Wenzel, T. J. *NMR Shift Reagents*; CRC Press: Boca Raton, Florida, 1987. *Nuclear Magnetic Resonance Shift Reagents*; Sievers, R. A., Ed.; Academic: New York, 1973. Hofer, O. *Top. Stereochem.* **1976**, *9*, 111–197.

Table 2. ^{1}H NMR Data (δ, ppm) for Coordinatively Unsaturated Complexes 5[a]

compd	solvent	$C_5(CH_3)_5$	CHR and R	Z
5a	$CDCl_3$	1.78 (s, 15H)	3.32 (s, 2H)	7.61 (~d, $J \approx$ 8, 2H)
				7.23 (~d, $J \approx$ 8, 2H)
				2.37 (s, 3H)
	CD_2Cl_2[b]	1.81 (s, 15H)	3.25 (s, 2H)	7.65 (~d, $J \approx$ 8, 2H)
				7.37 (~d, $J \approx$ 8, 2H)
				2.41 (s, 3H)
	C_6D_6	1.25 (s, 15H)	3.78 (s, 2H)	7.73 (~d, $J \approx$ 8, 2H)
				6.78 (~d, $J \approx$ 8, 2H)
				1.91 (s, 3H)
5b	$CDCl_3$	1.70 (s, 15H)	3.63 (s, 2H)	7.24–7.38 (m, 5H)
				5.16 (s, 2H)
5c[c]	$CDCl_3$	1.72 (s, 15H)	3.59 (s, 2H)	2.13 (s, 3H)
5d	$CDCl_3$	1.73 (s, 15H)	3.52 (q, J = 7, 1H)	7.63 (d, J = 8, 2H)
			1.31 (d, J = 7, 3H)	7.20 (d, J = 8, 2H)
				2.36 (s, 3H)
	C_6D_6	1.23 (s, 15H)	3.96 (s, 2H)	7.18–7.23 (m, 2H)
				7.00–7.14 (m, 3H)
				5.14 (s, 2H)
5e	$CDCl_3$	1.44 (s, 15H)	4.26 (dd, J = 2.6, 6.0, 1H)	7.27–7.46 (m, 5H)[d]
			3.26 (dd, J = 6.0, 13.3, 1H)	7.08–7.16 (m, 3H)[d]
			2.97 (dd, J = 2.6, 13.3, 1H)	6.85–6.90 (m, 2H)[d]
				5.30 (d, J = 12.3, 1H)
				5.17 (d, J = 12.3, 1H)
5f	$CDCl_3$	1.84 (s, 15H)	4.60 (s, 1 H)	7.39 (~d, J $\approx$ 8, 2 H)
			6.98–7.08 (m, 5H)	~7.1[e]
				2.29 (s, 3H)

[a] Coupling constants in Hz, at 300 MHz at ambient probe temperature unless otherwise specified. Referenced to $CHCl_3$ = 7.24 and C_6HD_5 = 7.15 ppm, respectively. [b] 400 MHz, $CHDCl_2$ = 5.28 ppm. [c] Red solution. [d] Resonances include those from Z and R groups. [e] Resonance obscured by signals for R = Ph.

or **5f** with (*S*)-α-methylbenzylamine gave mixtures of amides **10a/10b** and **11a/11b**,[21] respectively, in ratios of at least 20:1, signifying ee of at least 90%. An alternative, more sensitive method, based on coordination of an enantiomerically pure primary amine to Ir in **5**, indicated that **5f** and **5d** were obtained with ee of at least 96% and 99%, respectively.[22]

Evidence for intramolecular interaction of the (formally) unsaturated Ir center with an amino acid side chain was sought. On the basis of normal NMR chemical shifts for the phenyl protons and carbons of **5f**, the possibility of C–H agostic[23] or η^2-coordination[24] of the phenyl substituent in **5f** seemed unlikely. Nevertheless, additional characterization of **5f**, which would also examine the general effect of a metallacycle substituent R on the geometry of the ring, was deemed desirable. The results of X-ray diffraction of a crystal of **5f**, obtained by vapor diffusion of petroleum ether into a xylenes solution, are presented in Figure 2 and Tables 5, 10 and 12. As in **5a**, the chelate ring is nearly planar (all five atoms are less than 0.018 Å from the mean chelate plane), although some distortion is suggested by the distances of the Cp* centroid and S (0.083 and 0.362 Å, respectively) from that plane. The configuration of the stereogenic center established by derivatization to **11a/b** was verified by refinement of the Rogers η parameter to a value of 1.06(2).[25] The perpendicular distance of the Ir atom from the mean plane of the C_6H_5 ring is only 0.22 Å, as required for agostic interation, but the distance between Ir and H(9pa), the nearest hydrogen of the C_6H_5 ring, is ca. 3.6 Å, which is further than the internuclear distance of metal and hydrogen in an unambiguous agostic interaction.[23] The orientation of the C_6H_5 ring, though favorable for agostic interaction with Ir, may simply be a manifestation of π-stacking. Regardless, the syn arrangement of C_6H_5 and $CH_3C_6H_4$ substituents (angle between mean planes 19°) is an interesting contrast to the anti arrangement proposed for structurally uncharacterized boron-derived Lewis acids based on **4** and related species.[8]

Coordination Chemistry of 5. The deep red color of solutions of **5** fades to yellow within seconds after addition of a phosphine, unhindered amine, or CO. From all evidence gathered so far, the color change is diagnostic for coordinative saturation in these systems. The resulting glycine-derived complexes **6a–c** display ^{1}H NMR signals (Tables 6 and 7) ascribable to two mutually coupled diastereotopic methylene protons, as expected for species containing a chiral center. Comparison of ν_{CO} = 1684 cm^{-1} for **5a** and ν_{CO} = 1650 cm^{-1} for the corresponding PMe_3 adduct **6a**–PMe_3 suggests reduced donation of electron density from O to Ir upon coordinative saturation. Further, whereas **5b** (ν_{CO} = 1672 cm^{-1}, br) shows a single set of resonances in its NMR spectrum at ambient temperatures, **6b**–PMe_3 (ν_{CO} = 1645 cm^{-1}, br) shows *two* sets of absorptions, which coalesce at elevated temperatures (ca. 90 °C at 400 MHz). The ratio of the two species is solvent-dependent, changing from 1.6:1 in $CDCl_3$ to 2.3:1 in d_8-toluene. These data point to the presence of rotameric forms of *N*-Cbz-substituted complex **6b**–PMe_3 which interconvert slowly enough on the NMR time scale at ambient temperatures so as to show two sets of sharp resonances. Significantly, under similar conditions NMR spectra of **5b** exhibit only one set of sharp resonances, considered to be additional evidence for effective competition by the unsaturated Ir with the carbonyl group for electron density from N. Although activation parameters for rotation of the Cbz group were not determined in this study, the qualitative difference between the behavior of **6b**-PMe_3 and **5b** resembles the difference between an acylated amine and an acylated pyrrole.[26]

(21) (a) Compounds **11a,b** are mentioned, but without detail: Clark, C. R.; Bouhadir, K.; Mayfield, C. A.; DeRuiter, J. *J. Chromatogr. Sci.* **1990**, *28*, 407–412. (b) Compound **10**: Herlinger, H.; Kleinmann, H.; Ugi, I. *Justus Liebigs Ann. Chem.* **1967**, *706*, 37–46.

(22) Grotjahn, D. B.; Joubran, C. *Tetrahedron: Asymmetry* **1995**, *6*, 745–752.

(23) Brookhart, M.; Green, M. L. H.; Wong, L.-L. *Prog. Inorg. Chem.* **1988**, *36*, 1–124. Crabtree, R. H.; Hamilton, D. G. *Adv. Organomet. Chem.* **1988**, *28*, 299–338.

(24) Li, C.-S.; Jou, D.-C.; Cheng, C.-H. *Organometallics* **1993**, *12*, 3945–3954 and references therein.

(25) Rogers, D. *Acta Crystallogr., Sect. A* **1981**, *A37*, 734–741.

(26) Stewart, W. E.; Siddall, T. H., III. *Chem. Rev.* **1970**, *70*, 517–551. Jackman, L. M. In *Dynamic Nuclear Magnetic Resonance Spectroscopy*; Jackman, L. M., Cotton, F. A., Eds.; Academic: New York, 1975; pp 203–252.

Table 3. ^{13}C NMR Data (δ, ppm) for Coordinatively Unsaturated Complexes 5[a]

complex	*C*=O	$C_5(CH_3)_5$	$C_5(CH_3)_5$	*C*HR	R and Z[b]
5a	186.0	87.7	9.9	52.9	143.2 (C), 136.3 (C), 129.7 (CH), 127.4 (CH), 21.2 (CH_3)
5b	187.3	87.3	9.7	53.7	161.0 (C), 137.0 (C), 128.6 (CH), 128.2 (CH), 128.2 (C), 22.0 (CH_3)
5c	187.3	87.8	9.8	55.1	177.6 (C), 22.0 (CH_3)
5d	189.2	87.7	9.8	59.8	142.8 (C), 139.0 (C), 129.5 (CH), 127.1 (CH), 23.0 (CH_3), 21.2 (CH_3)
5e	188.6	86.8	9.4	64.6[c]	160.4 (C), 137.5 (C), 137.1 (C), 130.7 (CH), 128.7 (CH), 128.3 (CH), 127.9 (CH), 126.1 (CH), 67.7,[c] 38.3
5f	186.2	88.0	9.9	68.0	142.4 (C), 138.5 (C), 138.1 (C), 129.0 (CH), 127.9 (CH), 127.4 (CH), 127.2 (CH), 126.8 (CH), 21.0 (CH_3)

[a] In $CDCl_3$, measured at ambient probe temperature at 75.5 MHz. Resonance for solvent = 77.00 ppm. [b] Assignments based on intensities and chemical shifts. [c] Assignments uncertain.

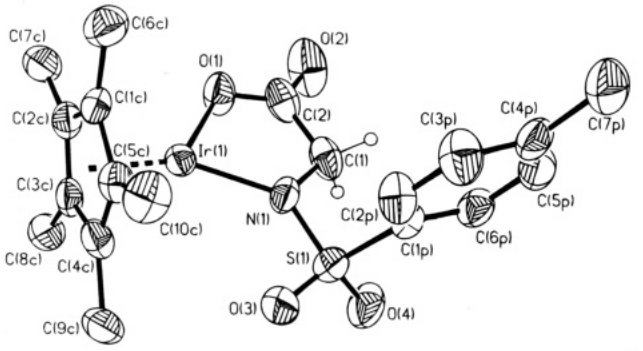

Figure 1. Molecular structure of **5a**, shown with 50% thermal ellipsoids. Hydrogen atoms other than those shown (assumed positions) are omitted for clarity.

Table 4. Bond Lengths (Å) and Selected Angles (deg) for 5a

Ir(1)–N(1)	1.981(7)	Ir(1)–O(1)	2.030(6)
Ir(1)–C(1C)	2.136(8)	Ir(1)–C(2C)	2.162(8)
Ir(1)–C(3C)	2.138(7)	Ir(1)–C(4C)	2.177(8)
Ir(1)–C(5C)	2.145(8)	N(1)–C(1)	1.485(11)
N(1)–S(1)	1.629(7)	C(1)–C(2)	1.513(14)
C(2)–O(1)	1.281(11)	C(2)–O(2)	1.222(12)
C(1C)–C(2C)	1.425(12)	C(1C)–C(5C)	1.455(12)
C(1C)–C(6C)	1.489(13)	C(2C)–C(3C)	1.401(11)
C(2C)–C(7C)	1.508(12)	C(3C)–C(4C)	1.460(12)
C(3C)–C(8C)	1.504(13)	C(4C)–C(5C)	1.415(11)
C(4C)–C(9C)	1.500(12)	C(5C)–C(10C)	1.501(12)
S(1)–O(3)	1.429(7)	S(1)–O(4)	1.450(7)
S(1)–C(1P)	1.786(9)	C(1P)–C(2P)	1.360(13)
C(1P)–C(6P)	1.373(13)	C(2P)–C(3P)	1.363(14)
C(3P)–C(4P)	1.395(14)	C(4P)–C(5P)	1.383(13)
C(4P)–C(7P)	1.502(14)	C(5P)–C(6P)	1.380(14)
N(1)–Ir(1)–O(1)	80.3(3)	C(1)–C(2)–O(2)	119.5(9)
Ir(1)–O(1)–C(2)	118.5(6)	Ir(1)–N(1)–S(1)	131.3(4)
O(1)–C(2)–C(1)	115.8(8)	C(1)–N(1)–S(1)	113.2(5)
C(2)–C(1)–N(1)	109.8(7)	N(1)–S(1)–C(1p)	105.3(4)
C(1)–N(1)–Ir(1)	115.3(5)	O(3)–S(1)–O(4)	118.7(4)
O(1)–C(2)–O(2)	124.6(9)		

Racemic **4g** and **2** afford yellow (±)-**8** (98% yield) directly, showing the possibility of side chain coordination. Two sets of resonances are seen in the ^1H NMR spectra of **8**. Because the ratio of the two species is 6:5 in $CDCl_3$ and 4:1 in C_6D_6, it is assumed that the difference between the two components is in the orientation of the Cbz group about the C–N bond and not in the undetermined configuration at S, which may in fact be changing rapidly on the NMR time scale at ambient probe temperature.[27]

Evaporation of a red solution of **5c** in CH_2Cl_2 (ν_{CO} = 1642, 1659 cm^{-1}) leaves a yellow solid (in KBr ν_{CO} = 1553, 1570, 1653 cm^{-1}) which redissolves rapidly to give a red solution in noncoordinating solvents. These properties are consistent with interconversion of red **5c** in solution and a yellow dimer or oligomer in the solid, with the former possibility being favored on the basis of literature precedents.[5b,28] In addition, whereas dissolution of **5c** in CH_2Cl_2 or THF affords a red solution, use of CH_3CN yields a pale orange solution, presumably containing CH_3CN complex **6c**–CH_3CN.

Table 5. Bond Lengths (Å) and Selected Angles (deg) for 5f

Ir(1)–N(1)	1.986(6)	Ir(1)–O(1)	2.022(9)
Ir(1)–C(1C)	2.135(15)	Ir(1)–C(2C)	2.168(8)
Ir(1)–C(3C)	2.125(9)	Ir(1)–C(4C)	2.149(8)
Ir(1)–C(5C)	2.154(9)	N(1)–C(1)	1.498(10)
N(1)–S(1)	1.634(6)	C(1)–C(2)	1.485(12)
C(1)–C(8P)	1.541(11)	C(2)–O(1)	1.280(12)
C(2)–O(2)	1.216(10)	C(1C)–C(2C)	1.395(17)
C(1C)–C(5C)	1.491(18)	C(1C)–C(6C)	1.506(18)
C(2C)–C(3C)	1.418(13)	C(2C)–C(7C)	1.528(14)
C(3C)–C(4C)	1.419(13)	C(3C)–C(8C)	1.486(16)
C(4C)–C(5C)	1.369(13)	C(4C)–C(9C)	1.485(14)
C(5C)–C(10C)	1.488(15)	S(1)–O(3)	1.449(10)
S(1)–O(4)	1.446(7)	S(1)–C(1P)	1.769(9)
C(1P)–C(2P)	1.383(14)	C(1P)–C(6P)	1.393(13)
C(2P)–C(3P)	1.420(15)	C(3P)–C(4P)	1.341(18)
C(4P)–C(5P)	1.371(18)	C(4P)–C(7P)	1.482(13)
C(5P)–C(6P)	1.427(14)	C(8P)–C(9P)	1.384(11)
C(8P)–C(13P)	1.380(12)	C(9P)–C(10P)	1.363(13)
C(10P)–C(11P)	1.315(18)	C(11P)–C(12P)	1.377(18)
C(12P)–C(13P)	1.429(16)		
N(1)–Ir(1)–O(1)	79.9(3)	C(1)–C(2)–O(2)	121.0(7)
Ir(1)–O(1)–C(2)	118.4(6)	Ir(1)–N(1)–S(1)	127.4(4)
O(1)–C(2)–C(1)	117.2(8)	C(1)–N(1)–S(1)	115.7(5)
C(2)–C(1)–N(1)	109.1(6)	N(1)–S(1)–C(1p)	108.3(4)
O(1)–N(1)–Ir(1)	115.4(4)	O(3)–S(1)–O(4)	117.5(4)
O(1)–C(2)–O(2)	121.8(8)		

Diastereoselectivity of Ligand Additions. It is anticipated that the stereochemical course of reactions at Ir in chiral **5** will depend on the diastereoselectivity of ligand additions to the metal. Addition of PMe_3 to a red solution of enantiomerically pure[22] (*S*)-alanine-derived complex **5d** within seconds gave a yellow solution, in which essentially a single set of sharp NMR resonances was seen. Integration established that the major product predominated over one or two minor components in a ratio of at least 25:1 (Table 8). NOE experiments indicated that, in the major product, the Cp* and alanine side chain CH_3 group are syn, and the PMe_3 and methine H are syn, as in structure **6d**–PMe_3. Similar color and spectral changes were observed when solutions of **5d–f** were treated with phosphines or CO. Moreover, NOE experiments on mixtures from **5d** + CO and **5f** + PMe_3 indicated a syn orientation of amino acid

(27) Reviews of the dynamics of coordinated thioethers: Jackson, W. G.; Sargeson, A. M. *Rearrange. Ground Excited States* **1980**, *2*, 273–378. Abel, E. W.; Bhargava, S. K.; Orrell, K. G. *Prog. Inorg. Chem.* **1984**, *32*, 1–118.

(28) Brown, L. D.; Itoh, K.; Suzuki, H.; Hirai, K.; Ibers, J. A. *J. Am. Chem. Soc.* **1978**, *100*, 8232–8238. Lindner, E.; Jansen, R.-M.; Mayer, H. A.; Hiller, W.; Fawzi, R. *Organometallics* **1989**, *8*, 2355–2360.

Table 6. ^{1}H NMR Data (δ, ppm) for PMe_3 Adducts 6–PMe_3 and 7–PMe_3[a]

compd	solvent	$C_5(CH_3)_5$	CHR and R	Z	L
6a–PMe_3	$CDCl_3$	1.69 (d, J = 2.1, 15H)	3.92 (d, J = 16.5, 1H) 3.67 (d, J = 16.5, 1H)	7.59 (~d, $J \approx 8$, 2H) 7.17 (~d, $J \approx 8$, 2H) 2.33 (s, 3H)	1.56 (d, J = 11.0, 9H)
6b–PMe_3	$CDCl_3$	major rotamer:[b] 1.53 (d, J = 2.0, 15H)	4.51 (d, J = 18.8, 1H) 3.84 (d, J = 18.8, 1H)	7.18–7.36 (m, 5H) 5.13 and 4.86 (two d, J = 11.5, each 1H)	1.26 (d, J = 10.7, 9H)
		minor rotamer:[b] 1.67 (d, J = 2.1, 15H)	4.48 (d, J = 18.5, 1H) 3.86 (d, J = 18.5, 1H)	7.18– 7.36 (m, 5H) 5.10 and 5.00 (two d, J = 12.8, each 1H)	1.41 (d, J = 10.9, 9H)
	d_8-toluene	major rotamer:[c] 1.34 (d, J = 2.0, 15H)	4.75 (d, J = 18.0, 1H) 4.06 (d, J = 18.0, 1H)	6.98–7.5[d] 5.23 and 5.20 (two d, J = 12.7, each 1H)	1.05 (d, J = 11.0, 9H)
		minor rotamer:[c] 1.18 (d, J = 2.1, 15H)	4.96 (d, J = 18.3, 1H) 3.08 (d, J = 18.3, 1H)	6.98–7.5[d] 5.26 and 4.84 (two d, J = 11.5, each 1H)	0.87 (d, J = 10.8, 9H)
6c–PMe_3	$CDCl_3$	1.67 (d, J = 2.6, 15H)	4.25 (d, J = 17.5, 1H) 3.94 (d, J = 17.5, 1H)	2.04 (s, 3H)	1.45 (d, J = 11.0, 9H)
6d–PMe_3	$CDCl_3$	1.69 (d, J = 2.1, 15H)	3.90 (q, J = 7.0, 1H) 0.99 (d, J = 7.0, 3H)	7.63 (~d, $J \approx 8$, 2H) 7.17 (~d, $J \approx 8$, 2H) 2.34 (s, 3H)	1.60 (d, J = 11.1, 9H)
6e–PMe_3	$CDCl_3$	major rotamer:[e] 1.49 (d, J = 2.2, 15H)	4.45 (dd, J = 3.9, 5.3, 1H)[f] 3.11 (dd, J = 3.9, 13.0, 1H)	7.02–7.42 (m, 10H)[f] 5.17 and 4.89 (two d, J = 11.6, each 1H)	1.21 (d, J = 10.7, 9H)
		minor rotamer:[e] 1.71 (d, J = 2.2, 15H)	4.46 (dd, J = 5.5, 6.9, 1H)[f]	7.02–7.42 (m, 10H)[f] 5.05 and 4.64 (two d, J = 12.4, each 1H)	1.36 (d, J = 10.9, 9H)
	d_8-toluene	major rotamer:[g] 1.39 (d, J = 2.1, 15H)	4.64 (dd, J = 4.4, 7.5, 1H)[f] 3.24 (dd, J = 7.5, 13.0, 1H) 3.13 (dd, J = 4.4, 13.0, 1H)	7.58 (d, J = 7.2, 2H)[f] 7.05–7.4 (m, 8H)[f] 5.21 and 4.94 (two d, J = 12.2, each 1H)	0.98 (d, J = 10.9, 9H)
		minor rotamer:[g] 1.16 (d, J = 2.0, 15H)	4.77 (dd, J = 3.4, 12.9, 1H)[f] 3.47 (dd, J = 7.5, 13.0, 1H) 3.36 (dd, J = 7.9, 12.9, 1H)	7.85 (d, J = 7.2, 2H)[f] 7.05–7.4 (m, 8H)[f] 5.25 and 4.88 (two d, J = 11.7, each 1H)	0.81 (d, J = 10.7, 9H)
7e–PMe_3	$CDCl_3$	major rotamer:[h] 1.55 (d, J = 2.1, 15H)	4.16 (dd, J = 2.1, 6.1, 1H)[f] 3.94 (dd, J = 6.1, 12.8, 1H)	7.25–7.4 (m, 5H)[f] 7.0–7.1 (m, 3H) 5.44 (d, J = 11.8, 1H) 4.58 (d, J = 11.8, 1H)	1.87 (d, J = 11.0, 9H)
		minor rotamer:[h,i] 1.57 (d, J = 2, 15H)	4.16	5.28 and 5.07 (two d, J = 11.6, each 1H)	1.21 (d, J = 11.0, 9H)
	C_6D_6	major rotamer:[j] 1.15 (d, J = 2.1, 15H)	4.47 (dd, J = 2.1, 6.2, 1H)[f] 4.63 (dd, J = 6.2, 12.3, 1H) 3.91 (dd, J = 2.1, 12.3, 1H)	7.95 (~d, J = 7, 2H)[f] 7.36 (~d, J = 7, 2H) 7.02–7.22 (m, 6H) 5.69 and 4.51 (two d, J = 11.9, each 1H)	0.59 (d, J = 10.9, 9H)
		minor rotamer:[i,j] 1.24 (d, J = 2, 15H)	4.37 (dd, J = 2, 5, 1H)[f] ~3.87[i] 3.68 (dd, J = 2, 12, 1H)	7.75 (~d, J = 7, 2H)[f] 7.49 (~d, J = 7, 2H) 7.02–7.22 (m, 6H) 5.51 and 5.21 (two d, J = 12.2, each 1H)	0.92 (d, J = 11.0, 9H)
6f–PMe_3	$CDCl_3$	1.70 (d, J = 2.1, 15H)	4.97 (s, 1H) 6.9–7.02 (m, 5H)	7.14 (~d, $J \approx 8$, 2H) 6.74 (~d, $J \approx 8$, 2H) 2.16 (s, 3H)	1.76 (d, J = 11.0, 9H)
	d_8-toluene	1.38 (d, J = 2.1, 15H)	5.28 (s, 1H) 7.2–7.27 (m, 2H) 6.9–6.96 (m, 3H)	7.47 (~d, $J \approx 8$, 2H) 6.57 (~d, $J \approx 8$, 2H) 1.91 (s, 3H)	1.50 (d, J = 11.0, 9H)

[a] Coupling constants in Hz, at 300 MHz at ambient probe temperature unless otherwise specified. [b] Ratio of rotamers 1.6:1. [c] Ratio of rotamers 2.3:1. [d] Resonances overlapping with those of solvent. [e] Ratio of rotamers 1.2:1. [f] Resonances for R = $PhCH_2$ overlap with those for Z = $PhCH_2CO_2$. [g] Ratio of rotamers 1.7:1. [h] Ratio of rotamers 5:1. [i] Some resonances for minor rotamer not found or overlap with others. [j] Ratio of rotamers 3:1.

side chain R and Cp* groups in the products, **6d**–CO and **6f**–PMe_3, respectively. Eventually (vide infra), an authentic sample of a diastereomer in which R and Cp* groups are trans to each other (**7e**–PMe_3) was synthesized independently, lending confidence to the assertion that **7e**–PMe_3 was not detectable (estimated 2% detection limit) in the addition of PMe_3 to **5d**.

All available evidence indicates that ligand attack on **5** is preferred from the side of the metallacycle unhindered by R. Evidence presented below indicates that this preference is the result of both kinetic and thermodynamic control.

Initial attempts to synthesize an authentic sample of the minor (or undetectable) diastereomer from ligand addition reactions focused on preparation of **7d**–PMe_3. Attempts to combine $Cp^*IrCl_2(PMe_3)$[29] (**12**) with **4d** using the conditions that worked in the synthesis of **5** (K_2CO_3, THF or MeCN) led to recovery of **12**, and use of Ag_2CO_3 as base slowly led to a mixture in which **6d**–PMe_3 was the only species identifiable by ^{1}H NMR as containing the $Cp^*Ir(PMe_3)$ and TsNCHMe– units.

(29) Isobe, K.; Bailey, P. M.; Maitlis, P. M. *J. Chem. Soc., Dalton Trans.* **1981**, 2003–2008.

Table 7. ^{1}H NMR Data (δ, ppm) for Coordinatively Saturated Complexes 6 and 7[a]

compd	solvent	$C_5(CH_3)_5$	CHR and R	Z	L
6d–PMe_2Ph	$CDCl_3$	1.45 (d, J = 2.2, 15H)	3.92 (q, J = 6.9, 1H) 1.00 (d, J = 6.9, 3H)	7.68 (~d, $J \approx$ 8, 2H) 7.19 (~d, $J \approx$ 8, 2H) 2.36 (s, 3H)	7.65–7.73 (m, 2H) 7.38–7.45 (m, 3H) 2.21 (d, J = 11.2, 3H) 1.56 (d, J = 11.1, 3H)
6d–$PMePh_2$[b]	$CDCl_3$	1.46 (d, J = 2.2, 15H)	3.75 (q, J = 7.0, 1H) 1.27 (d, J = 7.0, 3H)	7.13 (d, J = 8.2, 2H) 6.88 (d, J = 8.2, 2H) 2.23 (s, 3H)	7.90 (ddd, J = 11.6, 7.9, 2, 2H) 7.46–7.60 (m, 5H) 7.30–7.36 (m, 3H) 1.64 (d, J = 10.3, 3H)
7d–$PMePh_2$[b,c]	$CDCl_3$	1.49 (d, J = 2.4, 15H)	0.83 (d, J = 6.8, 3H)[c]	6.93 (d, J = 8.4, 2H) 6.77 (d, J = 8.4, 2H) 2.12 (s, 3H)	1.91 (d, J = 10.3, 3H)[c]
6a–PPh_3	$CDCl_3$	1.46 (d, J = 2.2, 15H)	3.82 (d, J = 16.5, 1H) 3.00 (d, J = 16.5, 1H)	7.01 (d, J = 8.2, 1H) 6.89 (d, J = 8.2, 1H) 2.26 (s, 3H)	6.9–7.8 (broad featureless resonances, 15H)
6d–PPh_3[d]	$CDCl_3$	1.50 (d, J = 2, 15H)	3.40 (q, J = 6.8, 1H) 1.46 (d, J = 6.8, 3H)	6.99 (d, J = 8, 2H) 6.88 (d, J = 8, 2H) 2.27 (s, 3H)	6.7–7.8 (broad)
7d–PPh_3[d]	$CDCl_3$	1.45 (d, J = 2, 15H)	4.05 (q, J = 7.0, 1H) 0.70 (d, J = 7.0, 3H)	6.84 (d, J = 8, 2H) 6.77 (d, J = 8, 2H) 2.24 (s, 3H)	6.7–7.8 (broad)
6a–CO	$CDCl_3$	1.91 (s, 15H)	3.76 (d, J = 16.6, 1H) 3.51 (d, J = 16.6, 1H)	7.65 (d, J = 8.2, 2H) 7.22 (d, J = 8.2, 2H) 2.37 (s, 3H)	
6d–CO	$CDCl_3$	1.89 (s, 15H)	4.04 (q, J = 7.0, 1H) 1.10 (d, J = 7.0, 3H)	7.67 (d, J = 8.2, 2H) 7.21 (d, J = 8.2, 2H) 2.36 (s, 3H)	
6d–$PhCH_2NH_2$[e]	$CDCl_3$	1.69 (s, 15H)	3.95 (q, J = 7) 0.90 (d, J = 7)	7.63 (d, J = 8) 7.19 (d, J = 8) 2.37 (s, 3H)	3.8–4.6 (br) 7.25–7.38 (m, 5H) 3.98 (br s, 2H)
6d–$PhCH_2NH_2$[f]	$CDCl_3$	1.61 (s, 15H)	3.94 (q, J = 7, 1H) 0.78 (d, J = 7, 3H)	7.63 (d, J = 8, 2H) 7.22 (d, J = 8, 2H) 2.38 (s, 3H)	7.25–7.38 (m, 5H) 4.52 (br s, 1H) 4.21 (br t, $J \approx$ 11, 1H) 4.08 (dt, J = 2, 12) ~3.94 (obscured by CHR)
6f–$PhCH_2NH_2$	$CDCl_3$	1.60 (s, 15H)	5.0 (s) and see L	7.46 (d, J = 8, 2H) 6.94 (d, J = 8, 2H) 2.23 (s, 3H)	7.26–7.36 (m, 5H) 6.96–7.02 (m, 5H) 4.03 (sl br s, 2H)
(±)-**6d**–$tBuNH_2$[g]	$CDCl_3$	1.68 (s, 15H)	3.67 (q, J = 6.9, 1H) 1.15 (d, J = 6.9, 3H)	7.63 (d, J = 7.9, 2H) 7.21 (d, J = 7.9, 2H) 2.36 (s, 3H)	1.19 (s, 9H)
(±)-**6d**–$tBuNH_2$[g,h]	$CDCl_3$	1.64 (s, 15H)	3.64 (q, J = 7, 1H) 1.10 (d, J = 7, 3H)	7.60 (d, J = 7.5, 2H) 7.23 (d, J = 7.5, 2H) 2.36 (s, 3H)	4.33 (d, J = 12, 1H) ~3.6 1.20 (s, 9H)
(±)-**6d**–DMAP[g,i,j]	$CDCl_3$	(s, 15H)			
(±)-**6d**–DMAP[g,i,k]	$CDCl_3$	1.55 (s, 15H)	3.59 (q, J = 7, 1H) 1.28 (d, J = 7, 3H)	7.09 (d, J = 8, 2H) 6.90 (d, J = 8, 2H) 2.20 (s, 3H)	8.32 (d, J = 6, 2H) 6.32 (d, J = 6, 2H) 3.03 (s, 6H)
(±)-**7d**–DMAP[g,i,k]	$CDCl_3$	1.33 (s, 15H)	4.02 (q, J = 7, 1H) 0.56 (d, J = 7, 3H)	7.56 (d, J = 8, 2H) 7.15 (d, J = 8, 2H) 2.33 (s, 3H)	8.17 (d, J = 6, 2H) 6.48 (d, J = 6, 2H) 3.09 (s, 3H)

[a] Coupling constants in Hz, at 300 MHz at ambient probe temperature unless otherwise specified. [b] Ratio of **6d**–$PMePh_2$ to **7d**–$PMePh_2$, ca 20:1. [c] Some resonances for minor diastereomer not found or assumed to overlap with others. [d] Ratio of **6d**–PPh_3 to **7d**–PPh_3, 6:1. Spectrum acquired at 63 °C at 500 MHz. At 25 °C, resonances for aryl protons of Ts in minor component were too broad to be discernible. [e] At 400 MHz. [f] At 400 MHz, −50 °C. [g] From racemic **5d**. [h] At 500 MHz, −50 °C. [i] Ratio of **6d**–DMAP to **7d**–DMAP, 6:1. [j] At 500 MHz. [k] At 500 MHz, −60 °C.

Alternatively, the dipotassium salt of **4d** was combined with $Cp^*Ir(OTf)_2(PMe_3)$[30] to give a mixture of products including **6d**–PMe_3 and several other Cp^*IrPMe_3-containing species, as suggested by the appearance of doublets in the region δ 0.5–2 ppm. Neither crystallization nor chromatography allowed the isolation of significantly purified material from these experiments. Fortunately, the synthesis of **7e**–PMe_3 from **12** and **4e** under standard conditions (K_2CO_3, MeCN) proved staightforward, giving **6e**–PMe_3 and another compound in a ratio of 1:4 (total 98% yield). The success of this latter reaction may be attributed to greater basicity (and presumably nucleophilicity) of the deprotonated carbamate moiety compared with the sulfonamide analog. ^{1}H NMR spectral data for the major product suggested that it had the same composition as **6e**–PMe_3, and the yellow compound could be isolated in a pure form (60%–67% yield) by fractional crystallization. All analytical data point to structure **7e**–PMe_3 as a mixture of two rotamers. Significantly, the resonances observed for the new compound were not detectable (estimated lower limit of sensitivity, 2%) in the spectrum of the reaction of **5d** with PMe_3.

The isolation of both diastereomers **6e**–PMe_3 and **7e**–PMe_3 allowed evaluation of thermodynamic and kinetic control of ligand binding. Heating a solution of **7e**–PMe_3 in C_6D_6 at 80 °C led to a smooth conversion (half-life = ca. 14 h) to **6e**–PMe_3, a process that was first-order in [**7e**–PMe_3] over at least 3 half-lives. Similar behavior at 90 °C (half-life = 5 h) was seen, and the final ratio of **6e**–PMe_3 to **7e**–PMe_3 was found to be 40:1, corresponding to a free energy difference of 2.7 kcal

(30) Stang, P. J.; Huang, Y.-H.; Arif, A. M. *Organometallics* **1992**, *11*, 231–237.

Table 8. ^{13}C NMR Data (δ, ppm) for Coordinatively Saturated Complexes 6[a]

complex	C=O	$C_5(CH_3)_5$	$C_5(CH_3)_3$	CHR	L	R and Z
6a−PMe_3	185.1	91.3 (d, J = 2.3)	9.3	52.9	13.8 (d, J = 37.8)	141.4, 139.7, 129.2, 127.0, 21.1
6b−PMe_3[b]	186.1 185.4	90.7 (d, J = 3.8, m) 90.5 (d, J = 3.4, M)	8.85 (m) 8.64 (M)	53.7 (M) 52.8 (m)	13.4 (d, J = 37, m) 12.6 (d, J = 37, M)	159.5 (C = O, M), 157.4 (C = O, m), 138.9, 138.1, 130.1, 128.6, 128.4, 128.3, 127.4, 67.0 (M), 66.2 (m)
6c−PMe_3	185.3	90.5 (d, J = 3)	8.94	55.5	13.4 (d, J = 37)	172.3 (C = O), 22.3 (CH_3)
6d−PMe_3	188.4	91.3	9.3	57.8	14.2 (d, J = 37)	141.5, 140.4, 129.2, 127.4, 21.1, 20.3
6e−PMe_3[c]	187.1 186.3	90.53 (d, J = 3) 90.45 (d, J =3)	9.1, 8.7	65.2,[d] 64.3[d]	13.2 (d, J = 36) 13.0 (d, J = 36)	140.1, 139.8, 138.6, 138.3, 130.4, 130.1, 129.9, 128.6, 128.3, 128.05, 128.01, 127.4, 125.93, 125.87, 66.8[d], 66.3[d], 42.9, 41.2
6d−PMe_2Ph	188.6	91.5 (d, J = 3)	8.8	57.5	135.0 (d, J = 54, C) 130.9 (d, J = 10, CH) 130.7 (d, J = 3, CH) 128.5 (d, J = 10, CH) 14.4 (d, J = 36) 11.3 (d, J = 36)	141.7 (C), 139.9 (C), 129.3 (CH), 127.6 (CH), 21.2 (CH_3), 20.7 (CH_3)
6d−$PMePh_2$	188.4	92.3 (d, J = 3)	8.9	58.0	135.3 (d, J = 11.9), 132.1 (d, J = 9.2), 131.7 (d, J = 2), 130.4 (d, J = 2), 128.6 (d, J = 11.0), 128.3 (d, J = 11.1), 13.6 (d, J = 36)	140.9 (C), 139.3 (C), 128.8 (CH), 127.4 (CH), 21.3 (CH_3), 21.0 (CH_3) 21.3[d]
6d−PPh_3	185.5	92.7 (d, J = 3)	9.1	52.18	134−136 (br), 130.6−132.4 (br), 128.2 (sl br d, J = 10)	140.5 (C), 138.6 (C), 127.1 (CH), 21.0 (CH_3)
6a−CO	185.0	100.9	9.0	53.9	169.2	142.7 (C), 135.9 (C), 129.7 (CH), 128.1 (CH), 21.2 (CH_3)
6d−CO	188.5	100.5	9.0	58.1	169.5	142.6 (C), 135.6 (C), 129.7 (CH), 128.0 (CH), 22.9,[a] 21.2 (CH_3)[d]
6d−$PhCH_2NH_2$	188.0	84.5	9.2	57.2	49.6 (br, NCH_2)	*e*, *f*
6d−$PhCH_2NH_2$[g]	187.9	84.1	9.3	56.7	50.0 (NCH_2)	*e*, *h*
6f−$PhCH_2NH_2$	185.6	84.6	9.0	64.3	49.4[e,i] (br, NCH_2)	21.1[e,i]
(±)-**6d**−$tBuNH_2$[g]	186.9	84.3	9.6	58.6	76.5 (NC), 31.0 (CH_3)	142.0, 137.2, 129.3, 127.0, 21.5, 19.7
6a−MeIm	185.1	84.8	9.0	52.5	34.4 (NCH_3)[e,j]	21.1[e,j]

[a] In $CDCl_3$, measured at ambient probe temperature at 75.5 MHz. Referenced to $^{13}CDCl_3$ = 77.00 ppm. Coupling constants in Hz. [b] Where possible, peaks assigned to major (M) and minor (m) rotamer (ratio, 1.6:1) based on signal intensity. [c] Two rotamers, ratio 1.2:1. [d] Assignment uncertain. [e] Other resonances could not be assigned to L, R, and Z with certainty. [f] 142.0, 139.6, 129.5, 129.3, 128.3 (br), 127.7, 21.2, 20.1. [g] At −50 °C and 125.7 MHz. [h] 141.8, 138.7, 138.5, 129.2, 128.9, 128.5, 128.1, 127.3, 21.6, 20.0. [i] 141.7, 141.0, 139.2, 129.3, 129.0, 128.34, (br), 128.28 (br), 127.9, 127.54, 127.50, 126.5. [j] 141.0, 140.3, 138.8, 130.1, 129.1, 127.1, 121.1.

Table 9. Diastereoselectivity of Ligand Addition Reactions on 5

reactants			
complex	ligand	ratio of **6**:**7**	ligand cone angle[a]
5d	PMe_3	≥25:1	118
5d	PMe_2Ph	≥25:11	122
5d	$PMePh_2$	20:1	136
5d	PPh_3	6:1	145
5d	CO	≥50:1	~95
5e	PMe_3	≥50:1	118
5f	PMe_3	≥50:1	118

[a] Reference 33a.

mol^{-1} at 90 °C. At 80 °C, the observed rate constant, $-0.044\ h^{-1}$, was unaltered within experimental uncertainty in separate experiments conducted in the presence of added PMe_3 (1.0 equiv) or **5b** (0.54 equiv), but in the early stages of the latter experiment, as the amount of **7e**−PMe_3 decreased, **6b**−PMe_3 was formed at the expense of **6e**−PMe_3. That isomerization involved inversion at Ir and not C was verified by the derivatization of the **6e**−PMe_3 produced in these experiments to amides **10a/b**, isolated in a ratio of at least 25:1. All results are consistent with isomerization of **7e**−PMe_3 via **5e** and free PMe_3.

The addition of PPh_3 to **5a** produced a yellow solution whose NMR spectrum exhibited sharp lines for all resonances except those attributable to the aryl protons of the PPh_3 ligand in **6a**−PPh_3. NMR spectra of the yellow solution produced by adding PPh_3 to chiral **5d** showed two sets of resonances in a ratio of 6:1 at ambient temperature and at 63 °C. At the lower temperature, the resonances assigned to the PPh_3 ligand were very broad, but were sharpened somewhat at the higher temperature. The two apparent doublets for the AA'XX' spin system of the tosyl group of the minor component were only visible at 63 °C. Because of the smooth decrease in selectivity with increasing phosphine size in Table 9, it is assumed that the predominant isomer from reaction of **5d** and PPh_3 is **6d**−PPh_3. In addition, rapid exchange of the bulky PPh_3 ligand was demonstrated by adding **5a** to a solution of **6d**−PPh_3 and **7d**−PPh_3 and observing within minutes the appearance of signals for **6a**−PPh_3 and **5d**.

Red solutions of **5** turn yellow on addition of a variety of primary aliphatic and heterocyclic amines, and decreased values for ν_{CO} as well as changes in NMR spectra are consistent with amine complexation to Ir to produce single diastereomers. In most cases, broadened resonances, especially those ascribable to protons on the amine nitrogen and on the carbon adjacent to it,

Table 10. Experimental Data for X-ray Diffraction Study of 5a and 5f

compd	**5a**	**5f**
empirical formula	$C_{19}H_{24}IrNO_4S$	$C_{25}H_{28}IrNO_4S$
color and habit	ruby red needle	ruby red parallelepiped
cryst size (mm^3)	0.10 × 0.15 × 0.45	0.15 × 0.25 × 0.30
cryst syst	monoclinic	monoclinic
space group	$P2_1/n$	$P2_1$
unit cell dimens	a = 7.2900(10) Å	a = 8.221(3) Å
	b = 12.137(2) Å	b = 9.435(3) Å
	c = 22.119(4) Å	c = 15.896(5) Å
	β = 91.88(3)°	β = 91.03(3)°
volume	1955.9(10) $Å^3$	1232.8(7) $Å^3$
Z	4	2
fw	554.7	630.7
density (calcd)	1.884 Mg/m^3	1.699 Mg/m^3
abs coeff	6.956 mm^{-1}	5.530 mm^{-1}
F(000)	1080	620
radiation	Mo Kα (graphite monochromated, λ = 0.710 73 Å)	
temp (K)	298	298
2θ range	3.5°–50.0°	3.5°–50.0°
scan type	ω	ω
scan speed	variable; 1.50°–14.65°/min in ω	variable; 1.50°–14.65°/min in ω
scan range (ω)	1.60°	1.60°
std reflns	3 measd every 47 reflns	3 measd every 47 reflns
index ranges	$-8 \le h \le 8, 0 \le k \le 14,$ $0 \le l \le 26$	$-9 \le h \le 9, -11 \le k \le 11,$ $-18 \le l \le 18$
reflns collected	3922	4810
indpdt reflns (%)	3467 (R_{int} = 1.90)	4810 (R_{int} = 6.65)
obsd reflns	2516 ($F > 4.0\sigma(F)$)	4252 ($F > 4.0\sigma(F)$)
absn corr	ψ-scan of 6 reflns	ψ-scan of 6 reflns
extincn corr	χ = −0.000 01(2), where $F^* = F[1 + 0.002\chi F^2/\sin(2\theta)]^{-1/4}$	0.000 00
hydrogen atoms	riding model, fixed isotropic U	riding model, fixed isotropic U
weighting scheme	$w^{-1} = \sigma^2(F) + 0.0004F^2$	$w^{-1} = \sigma^2(F) + 0.0010F^2$
no. of params refined	236	290
final R indices (obsd data, %)	R = 3.48, wR = 3.56	R = 2.99, wR = 3.77
R indices (all data)	R = 5.80, wR = 3.98	R = 3.65, wR = 3.99
goodness-of-fit	1.08	0.93
largest and mean Δ/σ	0.359, 0.002 (only nonzero Δ/σ was for extinction corr)	0.004, 0.000
data-to-param ratio	10.7:1	14.7:1
largest difference peak	1.16 e $Å^{-3}$ (6 largest peaks <1.3 Å from Ir1)	1.89 e $Å^{-3}$ (3 largest peaks <1) Å from Ir1)
largest difference hole	−0.87 e $Å^{-3}$	−0.92 e $Å^{-3}$

suggested that rapid amine exchange is rapid even at ambient probe temperature. Chemical evidence to confirm this suspicion came from addition of a second unsaturated complex **5a** to a solution of **6f**–$PhCH_2NH_2$: within time of mixing, a new species, tentatively identified as **6a**–$PhCH_2NH_2$, was present. The acquisition of NMR spectra of amine adducts at temperatures well below ambient allowed the resolution of even the protons on nitrogen; see Figure 3 for these observations on **6d**–$PhCH_2NH_2$.

The clean isomerization of **7e**–PMe_3 to **6e**–PMe_3 over hours at 80 °C described above would suggest that amines, which apparently exchange within minutes at room temperature, should bind so as to produce a thermodynamically preferred syn orientation of R and Cp* groups on the metallacycle. However, independent verification of this stereochemistry was sought through NOE experiments on amine adducts. The most successful of these attempts was performed at −60 °C on the mixture obtained from (±)-**5d** and DMAP (two isomers in a ratio of 6:1), giving results consistent with cis orientation of R = CH_3 and Cp* in the major component, (±)-**6d**–DMAP. The importance of steric requirements in amine binding was shown by Me_3N, which did not change the ^1H NMR spectrum or color of a solution of **5a** when added in equimolar amount, but when added in large excess (ca. 20 equiv) caused a color change to yellow and shifting of ^1H NMR signals.

Table 11. Atomic Coordinates (×10⁴) and Equivalent Isotropic Displacement Coefficients (Å² × 10³) for 5a

	x	y	z	U(eq)[a]
Ir(1)	1668(1)	780(1)	1607(1)	35(1)
N(1)	995(9)	2124(5)	1143(3)	41(2)
C(1)	−403(11)	2837(8)	1420(4)	51(3)
C(2)	−877(12)	2386(8)	2033(5)	55(3)
O(1)	−112(9)	1472(5)	2183(3)	56(2)
O(2)	−1989(9)	2874(6)	2337(4)	85(3)
C(1C)	3895(12)	−45(7)	2067(4)	41(3)
C(2C)	2277(11)	−687(7)	2131(3)	40(3)
C(3C)	1623(12)	−978(6)	1550(4)	41(3)
C(4C)	2876(11)	−561(7)	1102(4)	44(3)
C(5C)	4259(10)	33(7)	1425(4)	41(3)
C(6C)	5054(13)	465(8)	2558(4)	60(4)
C(7C)	1397(13)	−969(8)	2719(4)	53(3)
C(8C)	−61(13)	−1656(8)	1403(4)	57(3)
C(9C)	2729(14)	−787(8)	435(4)	60(3)
C(10C)	5921(12)	566(8)	1169(5)	61(4)
S(1)	1601(3)	2555(2)	481(1)	52(1)
O(3)	2810(10)	1749(5)	244(3)	64(3)
O(4)	−21(10)	2866(5)	124(3)	75(3)
C(1P)	2888(12)	3784(7)	625(4)	43(3)
C(2P)	4724(13)	3720(8)	749(4)	56(4)
C(3P)	5685(14)	4656(9)	885(5)	63(4)
C(4P)	4859(13)	5691(8)	912(4)	52(3)
C(5P)	3001(13)	5728(9)	766(4)	55(3)
C(6P)	2019(12)	4788(8)	619(4)	49(3)
C(7P)	5928(16)	6699(9)	1100(5)	77(5)

[a] Equivalent isotropic U defined as one-third of the trace of the orthogonalized U_{ij} tensor.

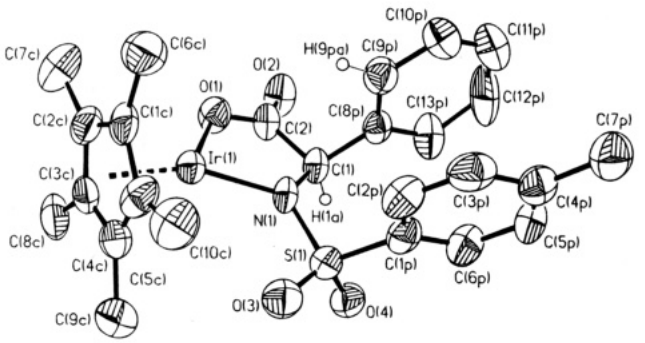

Figure 2. Molecular structure of **5f**, shown with 35% thermal ellipsoids. Hydrogen atoms other than those shown (assumed positions) are omitted for clarity.

Table 12. Atomic Coordinates ($\times 10^4$) and Equivalent Isotropic Displacement Coefficients (Å^2 $\times 10^3$) for 5f

	x	*y*	*z*	*U*(eq)[a]
Ir(1)	2186(1)	5000	1474(1)	47(1)
N(1)	2887(7)	3916(7)	2489(4)	50(2)
C(1)	3414(9)	2422(9)	2330(5)	53(2)
C(2)	3213(10)	2104(8)	1419(5)	58(3)
O(1)	2734(11)	3118(9)	940(5)	62(3)
O(2)	3511(9)	933(6)	1143(4)	79(2)
C(1C)	2724(17)	6916(15)	821(10)	72(5)
C(2C)	1629(12)	6144(10)	322(5)	65(3)
C(3C)	204(10)	5925(10)	795(5)	65(3)
C(4C)	384(10)	6638(9)	1577(6)	65(3)
C(5C)	1890(12)	7254(9)	1622(6)	69(3)
C(6C)	4423(14)	7404(12)	631(9)	103(5)
C(7C)	1870(18)	5504(15)	−550(7)	121(6)
C(8C)	−1222(11)	5098(24)	483(7)	99(4)
C(9C)	−929(13)	6777(12)	2202(7)	90(4)
C(10C)	2476(17)	8206(12)	2310(8)	105(5)
S(1)	2576(3)	4326(3)	3471(1)	57(1)
O(3)	1773(10)	5693(10)	3482(5)	85(3)
O(4)	1761(7)	3153(8)	3870(3)	71(2)
C(1P)	4489(11)	4509(9)	3988(5)	60(3)
C(2P)	5528(13)	5612(12)	3801(6)	80(4)
C(3P)	7049(12)	5670(14)	4236(7)	94(4)
C(4P)	7543(12)	4703(17)	4804(5)	83(5)
C(5P)	6519(13)	3597(14)	4975(6)	84(4)
C(6P)	4962(13)	3478(12)	4570(5)	79(3)
C(7P)	9149(11)	4767(24)	5240(6)	109(6)
C(8P)	5180(9)	2112(8)	2614(5)	54(2)
C(9P)	6469(10)	2951(10)	2370(5)	65(3)
C(10P)	8041(12)	2633(13)	2582(7)	84(4)
C(11P)	8419(13)	1542(15)	3061(8)	95(5)
C(12P)	7195(15)	632(13)	3290(8)	114(5)
C(13P)	5526(12)	928(10)	3096(6)	77(3)

[a] Equivalent isotropic *U* defined as one-third of the trace of the orthogonalized $\mathbf{U}_{ij}$ tensor.

Although comparative NMR data for diastereomers **6** and **7** are rather limited due to the pronounced tendency to form **6**, several generalizations may be made. Particularly instructive is comparison of complexes derived from **5d**, because of lack of complications due to rotamerism or other conformational effects in the corresponding adducts. Looking at ^{1}H NMR data for the pairs **6d**−/**7d**−$PMePh_2$, **6d**−/**7d**−DMAP, and **6d**−/**7d**−PPh_3 (Table 7), one sees two trends: the doublet ascribable to the alanine methyl group appears at significantly higher field in the **7d** series, whereas the quartet for the amino acid methine is found at lower field in the **7d** series. Attempts to extend this generalization to the better-characterized **6e**−/**7e**−PMe_3 pair seem to fail, presumably because of unknown influence of the CO_2CH_2Ph and CH_2Ph groups in their (presumably) different conformations. Regardless, the consistent trend seen for the **6d**−/**7d**−series lends confidence that the assigned stereochemistries are correct throughout.

Discussion

Stabilization of coordinatively unsaturated metal centers by heteroatom lone pair donation is now a well-established phenomenon,[15,16] and serves to explain the stability and bonding in **5**. Metallacycles related to **5** include **9**,[14] **13** (Scheme 2),[31a] **14**,[31b] and others which also feature essentially planar metallacyclic rings. An apparent exception was presented by **15**, which was reported to be coordinatively unsaturated, yet bent;[32a] subsequently, however, it was shown that intermolecular Ru−C contact was responsible for the distortion.[32b]

Among amino acid-derived complexes, the structurally characterized dimeric Cp*Rh−glycine *amide* complex **16** was suspected on the basis of ^{1}H NMR evidence of undergoing partial monomerization in solution to **17**, a species related to **5**, but formulated as rapidly epimerizing at Rh (**17a** + **17b**).[5b] Given our results, we suggest that **16** actually dissociates to form achiral structure **18**, a behavior reminiscent of the interconversion of red **5c** in solution and a yellow dimer or oligomer in the solid.

As far as we are aware, the only isolated coordinatively unsaturated amino acid complexes other than **5** are represented by structure **19**.[5a] These Rh(I) species undergo ligand substitution *and* addition to give bisphosphine or bisarsine complexes in which the two new ligands are presumably trans to each other, thus precluding an evaluation of asymmetric induction of ligand addition. Recently, dramatic enhancement of CO substitution in **21a** and **21b** compared to **21c** was explained by N-deprotonation and resulting stabilization of an otherwise undetected five-coordinate intermediate.[16k]

One unique feature of chiral **5** is the high stereoselectivity of ligand addition. Results presented above demonstrate that, for the small phosphine PMe_3, the selectivity is a result of both kinetic and thermodynamic control. Increasing the number of phenyl groups on the phosphine erodes selectivity to the point that the large phosphine PPh_3 adds with a selectivity of only 6:1. Moreover, the PPh_3 ligand, unlike PMe_3, exchanges readily even at ambient temperature. The more limited data on additions of amines to **5** seems to show a similar trend based on amine size, and the behavior of chiral **5** towards phosphines and amines may be explained by the cone angles of the ligands.[33]

On the basis of the experience of organic chemistry of cyclic compounds,[34] the kinetic preference for ligand approach to Ir in **5** from the side opposite the amino acid side chain R is understandable. Less obvious is the thermodynamic preference for a cis orientation of the two larger groups (Cp* and R) at the two stereogenic

(31) (a) Darensbourg, D. J.; Klausmeyer, K. K.; Mueller, B. L.; Reibenspies, J. H. *Angew. Chem., Int. Ed. Engl.* **1992**, *31*, 1503−1504. (b) Sellmann, D.; Wilke, M.; Knoch, F. *Inorg. Chem.* **1993**, *32*, 2534−2543. (c) Sellmann, D.; Ludwig, W.; Huttner, G.; Zsolnai, L. *J. Organomet. Chem.* **1985**, *294*, 199−207.

(32) (a) Kölle, U.; Kossakowski, J.; Raabe, G. *Angew. Chem., Int. Ed. Engl.* **1990**, *29*, 773−774. (b) Smith, M. E.; Hollander, F. E.; Andersen, R. A. *Angew. Chem., Int. Ed. Engl.* **1993**, *31*, 1294.

(33) (a) Tolman, C. A. *Chem. Rev.* **1977**, *77*, 313−348. (b) Seligson, A. L.; Trogler, W. C. *J. Am. Chem. Soc.* **1991**, *113*, 2520−2527.

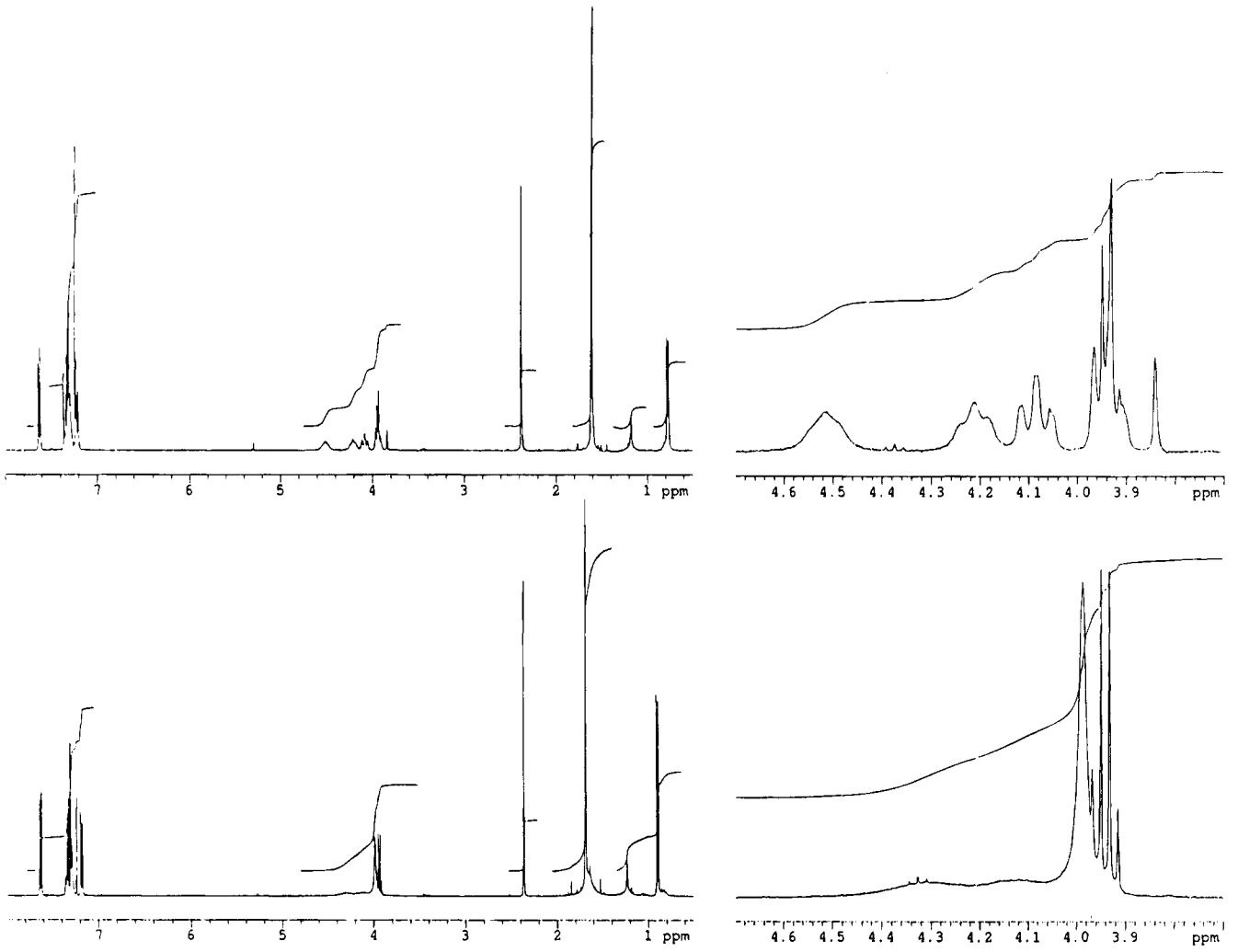

Figure 3. ^{1}H NMR spectra of **6d**–$PhCH_2NH_2$ ($CDCl_3$, 400 MHz) at −50 (upper) and 25 °C (lower).

centers. In this connection, we note that we have seen at least 50:1 thermodynamic preference for the cis isomer of **22** shown.[35] Presumably, the octahedral coordination environment about Ir in **6**, **7**, **22**, and related species makes the effective size of the metallacycle substituent L (in **6** or **7**) or chloride (in **22**) greater than that of Cp*, which is tilted further away from the stereogenic carbon.

Conclusions

Complexes **5** are unique coordinatively unsaturated derivatives of amino acids which enter into highly diastereoselective, rapid ligand addition reactions directed by steric interactions with nonpolar side chains, findings which we feel have relevance to design of both enantiomerically pure transition metal[3] and group 13[8] catalysts based on amino acids and related amides. Further applications of **5** and species related to it are under investigation.

Experimental Section

General. Amino acids were from commercial sources. Amino acid derivatives **4a**, **4d**, **4f**, and racemic **4g**[11] and iridium complexes **2**,[12] **12**,[29] and **14**[30] were synthesized according to published procedures. Amino acid derivatives **4b**,**c**,**e** were from commercial sources. Solvents CH_2Cl_2, CH_3CN, toluene, and hexanes were reagent grade and used as received, whereas THF and diethyl ether were freshly distilled from blue Na–benzophenone mixtures. Phosphines were purchased, with the exception of $PMePh_2$, which was prepared.[36] Unless otherwise specified, all reactions were conducted under nitrogen atmosphere, using Schlenk line techniques or in an M. Braun inert atmosphere glovebox.

NMR solvents (Cambridge Isotope Labs) C_6D_6, d_8-toluene, and CD_2Cl_2 were used as received, but $CDCl_3$ was passed through basic Al_2O_3 before dissolving organometallic complexes. Solvents for NMR tube reactions were degassed by three freeze–pump–thaw cycles. Resealable NMR tubes featuring a Teflon threaded cap were manufactured by J. Young, Ltd.

Infrared spectra were acquired on samples prepared in KBr pellets or as solutions held in NaCl cells. Either a Mattson Galaxy 2020 or a Nicolet 550 Magna FT-IR were used. NMR spectra were acquired at ambient probe temperatures of ca. 25 °C unless otherwise stated using a Varian Gemini 300, Unity Plus 400, Bruker 400, or Varian 500 MHz instrument. ^{1}H NMR spectra are referenced to residual solvent peaks (ppm): $CHCl_3$, 7.24; C_6HD_5, 7.15; $CHD_2C_6D_5$, 2.09; and $CHDCl_2$, 5.28, respectively. ^{13}C NMR spectra are referenced to $CDCl_3$

(34) For example, the addition of nucleophiles to cyclic ketones: Huryn, D. M. In *Comprehensive Organic Synthesis*; Schreiber, S. L., Ed.; Pergamon: Oxford, 1991; Vol. 1, Chapter 1.2, pp 49–75, especially pp 67–68.

(35) Grotjahn, D. B. Unpublished results; *Abstracts of Papers*, 208th National Meeting of the American Chemical Society, Washington, DC, August 1994; American Chemical Society: Washington, DC, 1994; ORGN 325.

(36) Bianco, V. D.; Doronzo, S. *Inorg. Synth.* **1976**, *16*, 155–161.

Scheme 2

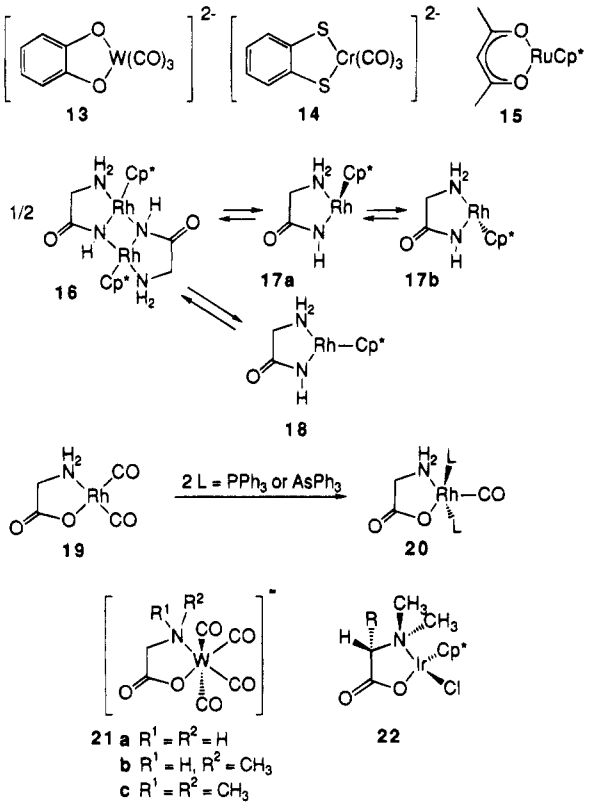

solvent resonance at δ 77.00 ppm. Elemental analyses were performed by Atlantic Microlabs, Norcross, GA.

Synthesis of 5a (Representative Procedure). Acetonitrile (10 mL) was added to $[Cp^*IrCl(\mu\text{-}Cl)]_2$ (**2**) (99.0 mg, 0.124 mmol), *N*-*p*-toluenesulfonylglycine (**4a**) (57.4 mg, 0.250 mmol), and anhydrous K_2CO_3 (72.8 mg, 0.527 mmol), and the resulting yellow mixture was deoxygenated by bubbling nitrogen through it for 10 min. After 5 h, the red mixture was concentrated by rotary evaporation. The residue was taken up in CH_2Cl_2 (10 mL) and filtered through a pad of Celite on a glass frit. The filter cake was rinsed with additional CH_2Cl_2 until filtrate was colorless. Combined filtrates were concentrated by rotary evaporation, and the red foamy residue was stored under high vacuum, leaving **5a** (133.8 mg, 97%).

The following compounds (**5b–f**) were isolated in a similar manner from the reactions indicated.

5b: From **2** (83.1 mg, 0.104 mmol), **4b** (43.9 mg, 0.210 mmol), and K_2CO_3 (66.8 mg, 0.483 mmol) stirred in THF (15 mL) for 0.7 days was obtained **5b** (105.0 mg, 94%) as a deep red solid.

5c (structure in solution): From **2** (104.9 mg, 0.1317 mmol), **4c** (30.7 mg, 0.2621 mmol), and K_2CO_3 (74.8 mg, 0.541 mmol) stirred in THF (10 mL) for 1.2 days was obtained a yellow solid (111.2 mg, 96%), identified as a dimer or oligomer of **5c**.

5d: From **2** (146.7 mg, 0.184 mmol), **4d** (89.8 mg, 0.369 mmol), and K_2CO_3 (102.5 mg, 0.742 mmol) in THF (18 mL), deoxygenated for 10 min and stirred at room temperature for 1.8 days, was obtained **5d** as a deep red powder (207.5 mg, 99%).

5e: From **2** (45.0 mg, 0.0565 mmol), **4e** (33.9 mg, 0.113 mmol), and K_2CO_3 (35.4 mg, 0.256 mmol) stirred in CH_3CN (3 mL) for 4 days was obtained **5e** (69.4 mg, 98%) as a deep red solid.

5f: From **2** (56.9 mg, 0.0714 mmol), **4f** (43.8 mg, 0.143 mmol), and K_2CO_3 (43.0 mg, 0.311 mmol) in CH_3CN (7 mL) stirred at room temperature for 6 h was obtained **5f** (86.5 mg, 96%) as a red foam.

Crystal Structures of 5a and 5f. Crystallization occurred from hot toluene (**5a**) or xylenes (**5f**) by diffusion with petroleum ether. Data were collected on a Siemens R3m/V autodiffractometer using graphite-monochromated Mo Kα radiation, see Table 10. The structures were solved by Patterson synthesis using SHELXTL/PC, and the resulting structural parameters were refined by least-squares techniques. Anisotropic thermal parameters were refined for all non-hydrogen atoms, and fixed thermal parameters were used for the included hydrogens.

Addition of PMe_3 to 5a To Produce 6a–PMe_3. A J. Young resealable NMR tube was charged with **5a** (13.9 mg, 0.0251 mmol). In the glovebox, deoxygenated $CDCl_3$ (1 mL) was filtered through basic Al_2O_3 into the NMR tube, and PMe_3 (2.8 μL, 0.027 mmol) was added, causing the red color of the solution to turn to yellow upon mixing. After observation of NMR spectra, the solution was transferred to a flask and concentrated by rotary evaporation, and the yellow residue was triturated under a little Et_2O and pentane. Removal of the supernatant by pipet and storage of the residue under high vacuum left **6a**–PMe_3 (14.1 mg, 89%) as a yellow powder. nOe experiments on the product in $CDCl_3$: Irradiation of the signal at δ 2.33 (Ar–CH_3) resulted in a 21% enhancement of the d at 7.17. Irradiation of the d at 1.56 ppm (PMe_3) produced enhancements in the d at 7.59 (3.6%), 3.92 (0.9%), and practically no change in the signal at 3.67 (0.05%). Irradiation of the d at 1.69 ppm (Cp*–CH_3) gave enhancements of the d at 7.59 (5.2%) and at 3.67 (1.8%) and led to a slight reduction of the d at 3.92 ppm (−0.3%), from which it was concluded that the methylene proton responsible for the d at 3.92 ppm is syn to PMe_3, whereas the proton resonating at 3.67 ppm is syn to Cp*.

6b–PMe_3: In the glovebox, PMe_3 (2.4 μL, 0.023 mmol) was added by syringe to a solution of **5b** (10.6 mg, 0.0198 mmol) in $CDCl_3$ (0.7 mL) in a J. Young resealable NMR tube, whereupon the red color of the solution faded to yellow. ^1H NMR showed two sets of signals, ascribed to a major and a minor rotamer in a ratio of 1.6:1.

6c–PMe_3: As in the preparation of **6b**–PMe_3, PMe_3 (1.6 μL, 0.015 mmol) was added by syringe to a solution of **5c** (6.6 mg, 0.015 mmol) in $CDCl_3$ (1 mL). $^{31}P\{^1H\}$ ($CDCl_3$, 202.3 MHz) −19.8 ppm.

6d–PMe_3: In the glovebox, $CDCl_3$ (1 mL) was filtered through basic Al_2O_3 (4 cm in a pipet) into a J. Young resealable NMR tube containing **5d** (20.5 mg, 0.0360 mmol). Trimethylphosphine (4.0 μL, 0.039 mmol) was added to the red solution, causing it to fade to yellow instantly. ^1H and $^{31}P\{^1H\}$ NMR spectra (the latter at 202.3 MHz, −17.0 ppm) indicated that a major compound was formed with a preponderance of at least 25:1 over minor, unidentified components as determined by integration of resonances in the range of δ 0.9–1.8 ppm. Concentration of the solution afforded **6d**–PMe_3 (22.0 mg, 95%) as a pale yellow solid.

6e–PMe_3: Following the preparation of **6a**–PMe_3, a solution of **5e** (11.9 mg, 0.190 mmol) in $CDCl_3$ (0.6 mL) was treated with PMe_3 (2.2 μL, 0.021 mmol), to give a solution of **6e**–PMe_3 as a mixture of two rotamers (1.2:1 in $CDCl_3$, 1.66:1 in d_8-toluene) as evidenced by two sets of sharp signals. $^{31}P\{^1H\}$ (C_6D_6, 161.9 MHz) −16.91 (major rotamer) and −17.37 (minor) ppm.

Synthesis of 7e–PMe_3. Acetonitrile (3.5 mL) was added to **4e** (10.5 mg, 0.0351 mmol), $Cp^*IrCl_2(PMe_3)$ (16.7 mg, 0.0352 mmol), and anhydrous K_2CO_3 (11.1 mg, 0.080 mmol) and N_2 was bubbled through the resulting yellow mixture for 5 min. After 1.8 days, the mixture was worked up as in the preparation of **5a**, leaving a pale yellow solid containing **7e**–PMe_3 and **6e**–PMe_3 (24.0 mg, 98%) in a ratio of 4:1 (^1H NMR). Recrystallization from THF–hexanes provided pure **7e**–PMe_3 (16.4 mg, 67%) as a pale yellow solid, existing as a mixture of rotamers in a ratio of 5:1 in $CDCl_3$ and 3:1 in C_6D_6. $^{31}P\{^1H\}$ (C_6D_6, 202.3 MHz) −23.33 (major rotamer) and −22.42 (minor) ppm.

NOE characterization of 6f–PMe_3 in $CDCl_3$. Irradiation of the multiplet at 6.9–7.02 ppm caused enhancement of

the resonances at 4.97 (13%) and 1.70 (1.0%) ppm. Irradiation of the singlet at 4.97 ppm led to enhancements of the signals at 7.14 (2.0%), 6.9–7.02 (2.6%), and 1.76 ppm (0.5%). Irradiation of the doublet at 1.76 ppm produced enhancement of the singlet at 4.97 ppm (12%), whereas irradiation of the doublet at 1.70 ppm led to insignificant enhancement of the singlet at 4.97 ppm (1.0%) and significant enhancement of the doublet at 7.14 (7.0%) and the multiplet at 6.9–7.02 ppm (4.6%). From these data it was concluded that the methine proton is syn to the PMe_3 ligand, whereas the Ph substituent is syn to Cp*.

6d–PMe_2Ph. From addition of PMe_2Ph (2.7 μL, 0.0190 mmol) to a solution of **5d** (10.5 mg, 0.0185 mmol) in $CDCl_3$ (1 mL) in the glovebox was obtained **6d**–PMe_2Ph (13.0 mg, quantitative) as a pale yellow powder. $^{31}P\{^1H\}$ ($CDCl_3$, 202.3 MHz) −12.0 ppm.

6d–$PMePh_2$. After $PMePh_2$ (6.1 μL, 0.0328 mmol) was added by syringe to a solution of **5d** (18.4 mg, 0.0324 mmol) in $CDCl_3$ (0.7 mL) in a J. Young NMR tube in the glovebox, the data reported in Tables 7 and 8 were obtained. The solution was poured through a plug of cotton in a pipet. The NMR tube and cotton were rinsed with CH_2Cl_2 in small portions, and the residue left from concentration of the combined filtrates was triturated with Et_2O–pentane. The supernatant was removed by pipet, and the remaining yellow powder was dried in vacuo over P_4O_{10} to leave **6d**–$PMePh_2$ (22.9 mg, 92%). $^{31}P\{^1H\}$ ($CDCl_3$, 202.3 MHz) 0.16 ppm. A small peak at −0.43 ppm may be due to **7d**–$PMePh_2$.

6a–PPh_3. A solution of **5a** (22.0 mg, 0.0397 mmol) and PPh_3 (10.8 mg, 0.0412 mmol) in an NMR tube in $CDCl_3$ was worked up as in the preparation of **6d**–$PMePh_2$ above to give **6a**–PPh_3 (31.6 mg, 97%). $^{31}P\{^1H\}$ ($CDCl_3$, 202.3 MHz) 12.97 ppm.

6d–PPh_3. As in the preparation of **6a**–PPh_3, **5d** (14.6 mg, 0.0257 mmol) and PPh_3 (6.8 mg, 0.0259 mmol) gave a solution containing two species in a ratio of 6:1. On the basis of results with other phosphines and **5d**, the major and minor components are presumed to be **6d**–PPh_3 and **7d**–PPh_3. Further workup left yellow powder (18.9 mg, 88%). $^{31}P\{^1H\}$ ($CDCl_3$, 202.3 MHz) 12.50 (**6d**–PPh_3) and 9.37 (**7d**–PPh_3) ppm.

6a–CO. $CDCl_3$ (1 mL) was filtered through basic Al_2O_3 (2 cm in pipet) onto **5a** (8.5 mg, 0.0153 mmol) in a resealable J. Young NMR tube. CO was bubbled though the red solution through a syringe needle for 2 min; the red color faded to pale yellow within the first few seconds. Nitrogen was bubbled through the solution for 2 min. ^1H and ^{13}C NMR spectra showed the presence of a single compound. Concentration of the solution left **6a**–CO (8.9 mg, quantitative) as a slightly orangish powder.

6d–CO. As in the preparation of **6a**–CO, **6d** (9.8 mg, 0.0172 mmol) and CO in $CDCl_3$ afforded a single compound, **6d**–CO, isolated as a pale orangish powder (9.2 mg, 90%).

(±)-6d-DMAP. Racemic **5d** (11.7 mg, 0.0205 mmol) and DMAP (2.4 mg, 0.0196 mmol) were dissolved in $CDCl_3$ (0.7 mL). ^1H NMR spectra showed a mixture of two components in the yellow solution both at ambient temperature (some peaks broadened) and at −60 °C. That DMAP exchange had been slowed sufficiently at −60 °C was shown by enhancement (0.6%) of the downfield doublet for the DMAP protons upon irradiation of the Cp* methyl resonance, and NOESY spectra showed a crosspeak between resonances ascribed to the Cp* methyl protons and H-2 and H-6 of DMAP. NOE experiments showed weak (0.06%) enhancement of the Cp* methyl protons on irradiation of the doublet ascribed to the alanine methyl group. Attempts at optimization of enhancements in this experiment and others on other amine adducts did not lead to more significant enhancements. Further workup as in preparation of **6d**–PMe_2Ph left (±)-**6d**–DMAP (14.5 mg).

(±)-8. A mixture of **2** (38.9 mg, 0.0488 mmol), (±)-**4g** (27.9 mg, 0.0984 mmol), and K_2CO_3 (36 mg, 0.26 mmol) in THF (10 mL) was stirred at room temperature. After 1 day, the mixture displayed a yellow color which remained unchanged. After a total of 3.5 days, the mixture was worked up as in the preparation of **5a** to afford (±)-**8** (58.3 mg, 98%) as a viscous yellow oil which slowly solidified. ^1H NMR [major and minor isomers (M and m) in a ratio of 6:5 in $CDCl_3$] δ 7.18–7.40 (m, 5 H for M + m), 5.28 (d, J = 12.0 Hz, 1 H for m), 5.04 and 5.07 (two d, J = 13.0 Hz, each 1 H for M), 4.86 (d, J = 12.0 Hz, 1 H for m), 4.66–4.73 (m, 1 H for M + m), 2.31 (s, 3 H for M), 2.1–2.35 (m, 2 H for M + m), 2.12 (s, 3 H for m), 1.69 (s, 15 H for M), 1.50 ppm (s, 15H for m); partial ^1H NMR [C_6D_6, major and minor rotamers (M and m) in a ratio of 4:1] δ 5.43 (d, J = 12.0 Hz, 1 H for m), 5.39 (d, J = 12.5 Hz, 1 H for M), 5.30–5.35 (m, 1 H for m), 5.21 (d, J = 12.5 Hz, 1 H for M), 5.06–5.12 (m, 1 H for M), 4.99 (d, J = 12.0 Hz, 1 H for m), 1.74 (s, 3 H for M), 1.55 (s, 3 H for m), 1.40 (s, 15 H for M), 1.12 ppm (s, 15 H for m); partial ^{13}C NMR ($CDCl_3$, 300 MHz) δ 186.4 and 185.6 (CCO_2), 159.7 and 157.6 (NCO_2), 138.6 and 138.3, 88.7 and 88.3, 66.4 and 66.2, 61.4 and 60.1, 8.7 and 8.5 ppm.

10b. Dichloromethane (10 mL) was added to DCC (140.9 mg, 0.683 mmol) and the (*R*)-enantiomer of **4e** (195.1 mg, 0.652 mmol), and the resulting mixture was stirred for 10 min before (*S*)-α-methylbenzylamine (81.0 mg, 0.668 mmol) was added using CH_2Cl_2 (2 × 1 mL). After 80 min, the mixture was concentrated to dryness, the residue was taken up in Et_2O, and the resulting mixture was filtered. The white filter cake was washed with Et_2O (total 50 mL, in portions), and the combined filtrates were concentrated, leaving 261 mg of crude product. Purification by radial chromatography over a 2 mm SiO_2 plate using EtOAc–petroleum ether (1:5 to 1:2) afforded **10b** (188.9 mg, 72%) as a white flaky solid. Mp 117.5–119.5 °C (lit. for enantiomer,[21b] 128–131 °C); ^1H NMR ($CDCl_3$, 300 MHz) δ 7.05–7.35 (m, 15 H), 5.68 (sl br d, J = 7.3 Hz, 1 H), 5.34 (br s, 1 H), 5.06 (s, 2 H), 4.95 (~quintet, $J \approx 7$ Hz, 1 H), 4.32 (~q, $J \approx 7$ Hz, 1 H), 3.15 (dd, J = 5.6, 13.5 Hz, 1 H), 2.94 (dd, J = 8.2, 13.5 Hz, 1 H), 1.225 ppm (d, J = 6.8 Hz, 3 H). Anal. Calcd for $C_{25}H_{26}N_2O_3$ (402.51): C, 74.60; H, 6.51; N, 6.96. Found: C, 74.73; H, 6.56; N, 6.95.

10a. By a procedure similar to that used for **10b**, **4e** (*S* configuration) (165.0 mg, 0.551 mmol), DCC (118.5 mg, 0.574 mmol), and (*S*)-α-methylbenzylamine (67.1 mg, 0.554 mmol) were reacted to produce **10a** (163.3 mg, 74%) as white solid. Significantly, **10a** exhibited the *same* R_f (0.6) as **10b** on SiO_2 (EtOAc–petroleum ether, 1:2) and therefore would not be expected to be chromatographically separated under the conditions used to remove some impurities in derivatization reactions. Mp 177–180 °C (lit.,[21b] 187–188 °C); IR (KBr) 3295 (br, NH), 1692 and 1648 cm^{-1} (C=O); ^1H NMR ($CDCl_3$, 300 MHz) δ 7.00–7.35 (m, 15 H), 5.79 (sl br d, J = 8 Hz, 1 H), 5.32 (br s, 1 H), 5.03 (d, J = 12.3 Hz, 1 H), 5.08 (d, J = 12.3 Hz, 1 H), 5.00 (quintet, J = 7.2 Hz, 1 H), 4.31 (~q, $J \approx 7$ Hz, 1 H), 3.07 (dd, J = 6.0, 13.6 Hz, 1 H), 2.95 (dd, J = 8.0, 13.6 Hz, 1 H), 1.35 ppm (d, J = 7.0 Hz, 3 H). Anal. Calcd for $C_{25}H_{26}N_2O_3$ (402.51): C, 74.60; H, 6.51; N, 6.96. Found: C, 74.02; H, 7.00; N, 7.33.

11a. Sulfonamide **4f** (280.0 mg, 0.917 mmol), HOBT (242.7 mg, 1.80 mmol), (*S*)-α-methylbenzylamine (115.3 mg, 0.951 mmol), and DCC (218.2 mg, 1.082 mmol) were allowed to react in THF. Chromatography and recrystallization afforded **11a** (351.2 mg, 94%) as a white solid. Mp 178–182 °C; IR (KBr) 3369, 3327, 3250 (N–H), 1656, 1644 (C=O) cm^{-1}; ^1H NMR ($CDCl_3$, 300 MHz) δ 7.56 (~d, $J \approx 8$ Hz, 2 H), 7.08–7.38 (m, 7 H), 6.10 (sl br d, $J \approx 8$ Hz, 1 H), 4.88 (d, J = 5.2 Hz, 1 H), 4.95 (~quintet, $J \approx 7$ Hz, 1 H), 4.75 (d, J = 5.2 Hz, 1H), 2.35 (s, 3 H), 1.29 ppm (d, J = 6.9 Hz). Anal. Calcd for $C_{23}H_{24}N_2O_3S$ (408.53): C, 67.62; H, 5.92; N, 6.86. Found: C, 67.34; H, 6.07; N, 7.05. A similar experiment starting with *racemic* **4f** afforded **11a** and **11b** in a ratio of 1:1 by ^1H NMR. In the ^1H NMR spectrum of the mixture, each of the four resonances in the region δ 4.7–6.1 and the doublet near 1.3 ppm appeared at different chemical shifts for **11a** and **11b**. The chemical shifts varied up to 0.1 ppm from sample to sample, but the chemical shift *differences* between resonances for **11a** and **11b**

did not change nearly as much, permitting determination of the ratio of the two diastereomers.

Example of the Determination of the Enantiopurity of 5. A solution of **5f** (27.6 mg, 0.0441 mmol) in CH_2Cl_2 (2 mL) was treated successively with MeOH (36 μL, 0.89 mmol) and Me_3SiCl (22 μL, 0.17 mmol), whereupon the solution turned orange. After 3 min, additional MeOH (2 mL) was added, followed by PPh_3 (11.9 mg, 0.0454 mmol; the presence of **2** seemed to interfere with subsequent reaction with (*S*)-α-methylbenzylamine, presumably by amine complexation). The mixture was concentrated, and the resulting residue (41 mg) was treated as in the preparation of **11a** with HOBT (12.6 mg, 0.0932 mmol), DCC (14.0 mg, 0.0679 mmol), and (S)-α-methylbenzylamine (5.8 μL, 0.0450 mmol) in THF (5 mL). The crude product after workup (41 mg) contained **11a** and DCU (^{1}H NMR), but peaks ascribable to **11b** could not be seen, indicating the presence of **11a** and **11b** in a ratio of at least 25:1.

Acknowledgment. We thank the Arizona State University Vice President for Research for partial support of this work, and Johnson Matthey Alfa/Aesar for a generous loan of iridium salts. Dr. Ron Nieman and Camil Joubran graciously performed NOE and VT NMR experiments, and the NSF (CHE-88-13109, CHE-92-14799, and BBS 88-04992) and Arizona State University provided funds for the requisite NMR instrumentation.

Supporting Information Available: Further details of the structure determinations of **5a** and **5f**, including a crystal-packing diagram for **5a** (64 pages). Ordering information is given on any current masthead page.

OM950028X